Accepted Article Preview: Published ahead of online publication

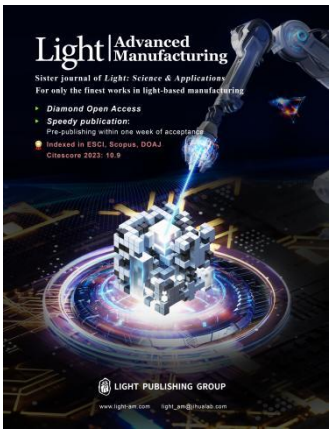

Structural Colour Engineering: From Precision Nanofabrication to Dynamic Modulation for Intelligent Surface Applications

Lin Zhang, Caixia Zhang, Yang Yang, Jieqiong Lin, Jiwang Yan

Cite this article as: Lin Zhang, Caixia Zhang, Yang Yang, Jieqiong Lin, Jiwang Yan. Structural Colour Engineering: From Precision Nanofabrication to Dynamic Modulation for Intelligent Surface Applications. *Light: Advanced Manufacturing* accepted article preview 24 June, 2026; doi: 10.37188/lam.2026.111

Received 15 October 2025; Revised 23 June 2026; Accepted 24 June 2026;
Accepted article preview online 24 June 2026

Structural Colour Engineering: From Precision Nanofabrication to Dynamic Modulation for Intelligent Surface Applications

Lin Zhang[a,b], Caixia Zhang[a,b], Yang Yang[c,*], Jieqiong Lin[a,b], Jiwang Yan[d,*]

a. Jilin Provincial Key Laboratory of Micro-Nano and Ultra-Precision Manufacturing, School of Mechatronic Engineering, Changchun University of Technology, Yan'an Ave 2055, Changchun, Jilin 130012, China

b. Jilin Provincial Key Laboratory of International Science and Technology Cooperation for High Performance Manufacturing and Testing, School of Mechatronic Engineering, Changchun University of Technology, Yan'an Ave 2055, Changchun, Jilin 130012, China

c. School of Intelligent Systems / School of Robotics and Advanced Manufacturing (Shenzhen), Harbin Institute of Technology Shenzhen, Shenzhen 518500, China

d. Department of Mechanical Engineering, Faculty of Science and Technology, Keio University, Hiyoshi 3-14-1, Kohoku-ku, Yokohama 223-8522, Japan

*Corresponding author: yangyang2020@hit.edu.cn (Y. Yang), yan@mech.keio.ac.jp (J. Yan)

Structural Colour Engineering: From Precision Nanofabrication to Dynamic Modulation for Intelligent Surface Applications

Abstract

Structural colour engineering, which involves the manipulation of light at the nanoscale, has emerged as a foundational technology for next-generation intelligent surfaces, moving beyond static displays to enable adaptive, interactive, and multifunctional applications. Emerging from engineered light-matter interactions, it represents a sustainable and dynamically tunable alternative to conventional pigments with transformative potential across advanced technologies. This review provides a comprehensive examination of recent breakthroughs in the nexus between nanofabrication and dynamic modulation technologies for structural colour engineering. Precision mechanical techniques, such as single-point diamond turning and elliptical vibration cutting, enable deterministic subwavelength optical control using programmable toolpaths. Conversely, nonmechanical approaches, such as multiphoton lithography and laser nanostructuring, facilitate the scalable production of functional metasurfaces. Dynamic systems achieve real-time spectral tuning across the visible spectrum through stimuli-responsive mechanisms, including strain-mediated grating reconfiguration and photothermally actuated nanocomposites. These paradigm-shifting advances underpin transformative applications in three key domains: adaptive optical camouflage with environmentally mimicking chromatic shifts, high-security anti-counterfeiting platforms featuring angularly encrypted imagery, and wearable biosensors. However, persistent challenges remain, particularly in reconciling nanoscale precision with industrial scalability, ensuring operational stability under multiphysics field coupling, and expanding the achievable colour spaces. By establishing fundamental connections among photonic design principles, nanofabrication innovations, and stimuli-responsive materials, this analysis outlines an interdisciplinary roadmap for next-generation intelligent surfaces. This ultimately underscores the unique capacity of structural colouration to enable not only

eco-friendly but also adaptive and interactive intelligent surface engineering solutions.

Keywords: structural colour, light-matter interactions, fabrication techniques, dynamic modulation, surface engineering

Abbreviations

SPDT	Single-point diamond turning	RFC	Radial fly cutting
DML	Diamond microlithography	SA-HFRFC	Servo-assisted helical feed radical fly cutting
FTS	Fast tool servo	UAUP	Ultrasound-assisted ultra-precision planarization
OVDs	Optical variable devices	NI-P	Nickel-phosphorus
MFVC	Multi-frequency vibratory cutting	ORUM	Oblique rotational ultrasonic milling
SVC	Shape vibration cutting	DNL	Dip-pen nanodisplacement lithography
UPC	Ultra-precision diamond cutting	TPL	Two-photon polymerization lithography
EVT	Elliptical vibratory turning	SMPs	Shape memory polymers
TMG	Tertiary motion generator	PPLL	Patterned pulsed laser lithography
EVC	Elliptical vibratory chiselling	LIPSSs	Laser-induced oxidation periodic surface structures
AFC	Axial feed fly cutting	SPR	Surface plasmon resonance
VAFC	Vibration-assisted fly cutting	DLW	Direct writing
LIG	Laser-induced graphene	MLA	Microlens array
CD	Compact disc	DRIE	Deep reactive ion etching
PDMS	Polydimethylsiloxane	BM	Brightness mechanochromism
SCP	Structural colour printing	HCM	Hue change mechanochromism
1DPCs	One-dimensional photonic crystals	VAM	Viewable angle mechanochromism
OPV	Organic photovoltaic technology	EVN	Elliptic vibration nanoimprint
NIL	Nanoimprint lithography	RIP	Resonant laser printing
EVC	Elliptical vibratory cutting	FCT	Fly cutting technology
UAM	Ultrasonic assisted machining		

Introduction

Colour is a fundamental visual phenomenon arising from the interaction of visible light with matter [1]. When light impinges on the surface of a material, its partial reflection, transmission, and absorption collectively govern the observed chromatic effects [2]. In nature, colour generation manifests through three primary mechanisms: chemical pigmentation, bioluminescence, and structural colouration. Historically, pigment-based solutions have dominated anthropogenic applications because of their versatility in art, industry, and daily commerce [3]. However, inherent limitations, such

as environmental persistence, non-recyclability, photodegradation, and pollution, compromise their sustainability [4]. In contrast, structural colouration generates hues through photon modulation using precisely engineered micro/nanoscale architectures, thus circumventing the need for molecular absorption-based pigments. This physical mechanism confers exceptional advantages such as superior photostability, environmental compatibility, and dynamic spectral tunability [5-7]. Consequently, recent breakthroughs in structural colour engineering have established it as a frontier research domain within materials science, offering sustainable alternatives that simultaneously address the ecological and durability constraints inherent to traditional colorants [8, 9].

The study of structural colour is deeply rooted in biological systems, where it plays a pivotal role in animal colouration and visual communication. As Cuthill *et al.* emphasised [10], evolutionary adaptations in animals integrate pigment utilisation, structural engineering, and functional principles to achieve colouration. Nature exemplifies structural colouration through hierarchically organised micro/nanostructures in butterfly wing scales [11], peacock feather ocelli [12], fish skin [13], and reptilian skin [14], which selectively manipulate light.

Notably, certain birds dynamically modulate feather colouration via nanostructural reconfiguration [15]. Species such as chameleons and cephalopods achieve real-time colour shifts through coordinated control of pigment distribution and nanostructural spacing, enabling adaptive camouflage, thermoregulation, and signalling. These biological paradigms of dynamic colour regulation have inspired breakthroughs in artificial structural colour engineering. By mimicking natural strategies, researchers have demonstrated stimuli-responsive systems capable of tunable optical properties, expanding applications in adaptive optical devices, information encryption, and biomimetic materials [16, 17].

Despite this progress, a critical gap remains: the translation of dynamic biological mechanisms into artificial systems lacks the seamless integration of multiscale structural design and practical scalability. This review addresses this gap by focusing

on the convergence of bio-inspired design, fabrication technologies, and dynamic modulation, an organizational perspective that links fundamental mechanisms to real-world applicability.

Structural colouration arises from periodic micro/nanostructures on material surfaces that selectively reflect specific wavelengths through light-matter interactions to generate diverse chromatic effects [18, 19]. The realisation of these architectures depends on two complementary fabrication paradigms: mechanical approaches (e.g., single-point diamond turning and vibration-assisted machining) enabling deterministic surface patterning, and nonmechanical techniques (e.g., laser ablation and photolithography) facilitating scalable metasurface production [20]. Both methods collectively support tailored colour modulation, while advancing cost-effective large-area manufacturing.

Critically, dynamic control of structural colours achieved by geometric reconfiguration of nanostructures, such as strain-induced lattice adjustments, enables real-time spectral tuning across the visible spectrum and accelerates adaptive optical systems [21, 22]. The functional versatility of structural colours spans optical communication devices, ultrasensitive biosensors, and high-security anti-counterfeiting technologies [23], while their integration with smart materials unlocks transformative applications in wearable electronics, energy-efficient displays, and responsive coatings [24-26].

However, key research gaps persist: the co-design of multiscale structures for synergistic optical performance, optimisation of environmental stability for long-term use, and scalable integration of dynamic modulation modules into practical devices remain underdeveloped. These gaps hinder the widespread commercialisation of structural colour technologies, making them a priority area for future research.

To provide a clear framework for this review, **Fig. 1** presents an overview of the core themes of fabrication technologies and dynamic modulation strategies. The figure adopts a three-ring structure; the innermost ring denotes the title of the review,

encapsulating the central focus on structural colour engineering. The middle ring is divided into three segments, corresponding to the core pillars of the review: mechanical processing, nonmechanical processing, and dynamic regulation. The outermost ring elaborates on each pillar using specific techniques: mechanical processing includes single-point diamond turning and vibration-assisted machining; non-mechanical processing includes laser processing and nanolithography; and dynamic regulation encompasses in situ stretching and tunable diffraction gratings. This visual framework contextualises the structure of the review and guides readers through the interconnections between fabrication methods and dynamic functionalities.

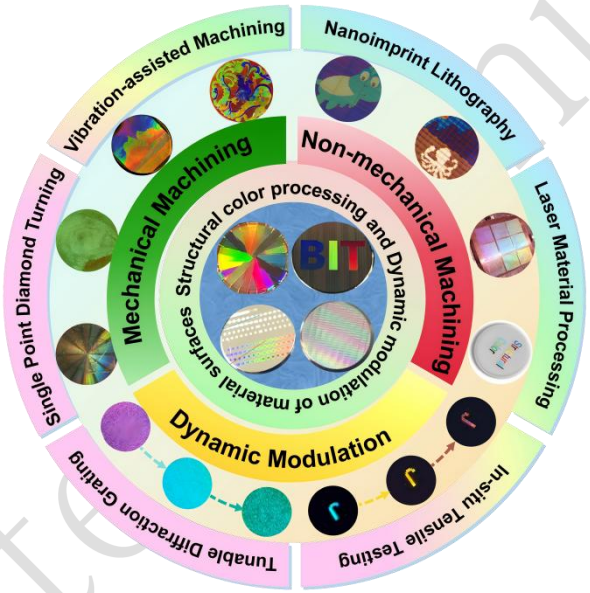

Fig. 1. Advances in structural colour research, including fabrication techniques and dynamic modulation.

This review systematically examines recent advances in structural colour research in materials science, focusing on micro/nanostructure fabrication methods and their applications in dynamic modulation techniques. Through a comparative analysis of existing technologies, we highlight the unique advantages of structural colour materials in optical sensing, adaptive displays, and smart material systems, while explicitly addressing the aforementioned research gaps.

The conclusion synthesises key findings and outlines prospects, emphasising the potential of structural colours in sustainable manufacturing and flexible electronics.

Fig. 2 presents the logical framework of this study. By targeting critical challenges such as multiscale structural co-design, environmental stability optimisation, and scalable integration, this review aims to accelerate the translation of structural colour technologies into high-precision optical devices and green energy applications, thereby driving innovation in next-generation materials science.

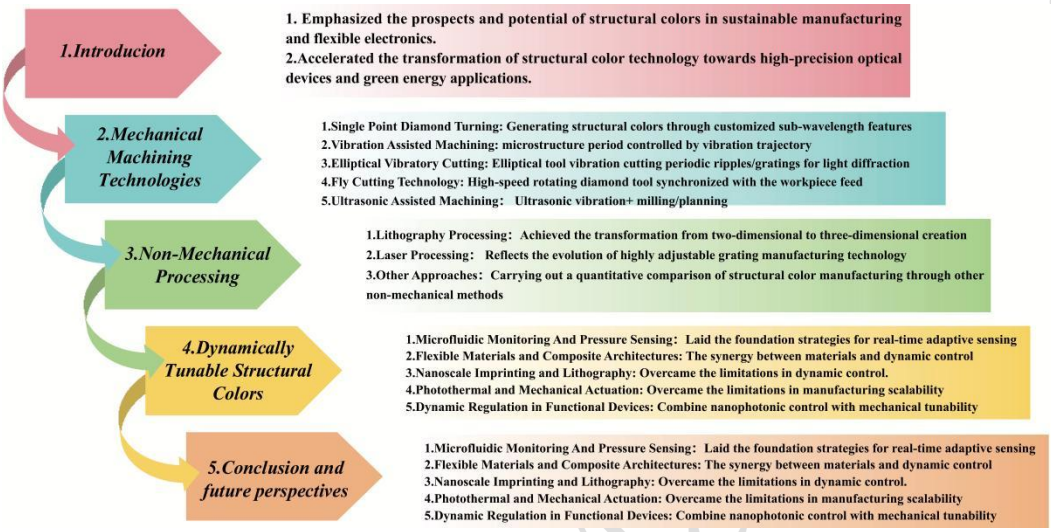

Fig. 2 Conceptual framework of the review.

Mechanical Machining Technologies

Mechanical machining technologies represent the cornerstone of structural colour manufacturing, delivering nanoscale control over surface micro/nanostructures to engineer tailored optical responses [27-30]. Key techniques, such as precision turning, fly cutting, planning, and milling, have been extensively developed, demonstrating exceptional capabilities in the deterministic fabrication of periodic architectures. These approaches enable diverse applications including high-resolution optical devices, dynamic anti-counterfeiting systems, and scalable metasurface production.

Single-Point Diamond Turning

Single-point diamond turning (SPDT) has emerged as a cornerstone technology for advanced optical surfaces, leveraging nanometer-scale accuracy and deterministic control over micro/nanostructures owing to the exceptional hardness of diamond tools and ultraprecision motion systems. This subtractive process enables the direct fabrication of complex 3D micro-structures, transcending the planar limitations of

conventional lithography via programmable toolpaths that regulate geometric parameters, such as height, curvature, and spatial period, for multidimensional wavefront engineering of phase, amplitude, and polarisation states.

Significant breakthroughs demonstrate the versatility of SPDT across material classes. In metals, Ding *et al.* [31] optimised ultrasonic-assisted SPDT to fabricate high-aspect-ratio aluminium micro-pillar arrays(~1.1×~1.3×~5.3 μm, aspect ratio~4.4) for photonic crystal devices. Similarly, Ding *et al.* achieved structural colour modulation through periodic micro-pillar arrays (12.8×15.8×28.2 μm, aspect ratio~1.8) on oxygen-free copper surfaces by SPDT, laying the foundation for next-generation display technologies, as shown in **Fig. 3A** [32].

For hard/brittle materials, Tang *et al.* [33] combined cryogenic SPDT with tool geometry optimisation on chalcogenide glass, achieving nanometric form accuracy (PV 120.82 nm) and sub-nm roughness(Ra 6.47 nm) for 15 mm-diameter aspheric lenses, whereas Cao *et al.* [34] surpassed critical depth-of-cut limits in SiC ceramics using ultrasonic assistance to produce supersmooth sawtooth structures (groove width ≥6 μm, depth up to 3.2 μm) for infrared optics, as shown in **Fig. 3B.**

The anisotropic nature of single-crystalline materials has been strategically exploited for functional modulation, as exemplified by To *et al.* [35], who attained ultrasmooth aluminium surfaces (RMS down to 4.2 nm) and polarisation-sensitive devices through crystallographic orientation control and anisotropic chip flow manipulation. Concurrently, Zhang *et al.* [36] achieved sub-micro shape accuracy (absolute error <3 μm) in spaceborne aspheric lenses via real-time force signal compensation.

This synergistic “material-process-function” co-innovation paradigm has propelled SPDT from conventional optical manufacturing to frontier applications in structural colouration and metasurfaces, thereby establishing a transformative technological pathway for next-generation photonic devices.

Diamond microlithography (DML) is a pivotal innovation in this field [37]. Its principle involves engraving micro-inverted pyramid arrays (aperture size 2.5-10 μm,

aspect ratio 0.41-0.59, cell pitch 10 μm) on a metal surface using a V-shaped diamond tool (nose radius below 1 μm, included angle 100°/120°), where each pyramid acts as a pixel. Grayscale is rendered by the difference in light reflection between these dark pyramids and the bright, unprocessed surface. The key to precision is the superposition projection algorithm (SPA), which converts a digital grayscale image into a spiral tool path for machining. These periodic microstructures facilitate wavelength-selective interference via diffraction, achieving up to 80% sRGB coverage. This mechanism provides exceptional durability and anti-counterfeiting utility by overcoming the photostability limits of chemical pigments (**Fig. 3C(a)-(c)**).

Subsequent advancements focused on the generation of freeform microstructures with enhanced functionality. Building on DML, Huang et al [38]. integrated an SPDT with a fast tool servo (FTS). Their methodology established a direct chain from a digital image to a 3D toolpath: a grayscale intensity matrix (resolution up to 1800 × 1519 pixels) is mapped onto an Archimedean spiral, with darker pixel values normalised to greater Z-axis heights (0-4μm) for FTS-based, real-time machining. This process enabled the fabrication of freeform features with a sample radius of 3 mm and sub-micron level surface precision, supporting the predictive "topography-optics" co-design of elements such as holographic security features by establishing a correlation between microstructure height and CIE-Lab colour parameters.

However, the path to industrial scalability faces significant challenges, primarily tool wear during high-speed FTS operations and edge chipping in brittle materials. To address these limitations, Li et al [39]. developed a data matrix-based SPDT process. This method explicitly correlates optical functionalities with machining parameters, utilising a 90° sharp-tip diamond tool to fabricate micro-groove arrays (pitch 50 μm, length 200 μm, depth 8.5-24 μm, slope angle 10°/44°) on RSA 905 substrates. By implementing optimised toolpaths (generated via MATLAB with ≥5 key points per groove) and precise process control, they achieved microstructures with a surface roughness of Sa=12 nm (for 10° grooves) and minimal burr height (3.6 ± 1.2 μm), delivering high-precision optical surfaces with distinguishable contrast between

orthogonal textured modules. This study demonstrated the potential of SPDT to evolve from creating passive structural colours to fabricating integrated, multifunctional optical systems incorporating elements such as waveguides and beam splitters.

Single-point diamond turning (SPDT) is a critical technology for structural colour engineering, enabling precise nanoscale fabrication of photonic devices from digital designs via tailored subwavelength features to produce durable structural colours for diverse applications (e.g., anti-counterfeiting, dual-function optics), while ongoing challenges in machining models, material damage, and throughput are expected to be addressed by advances in hybrid processing, artificial intelligence (AI), and sustainable materials to accelerate its industrial transition.

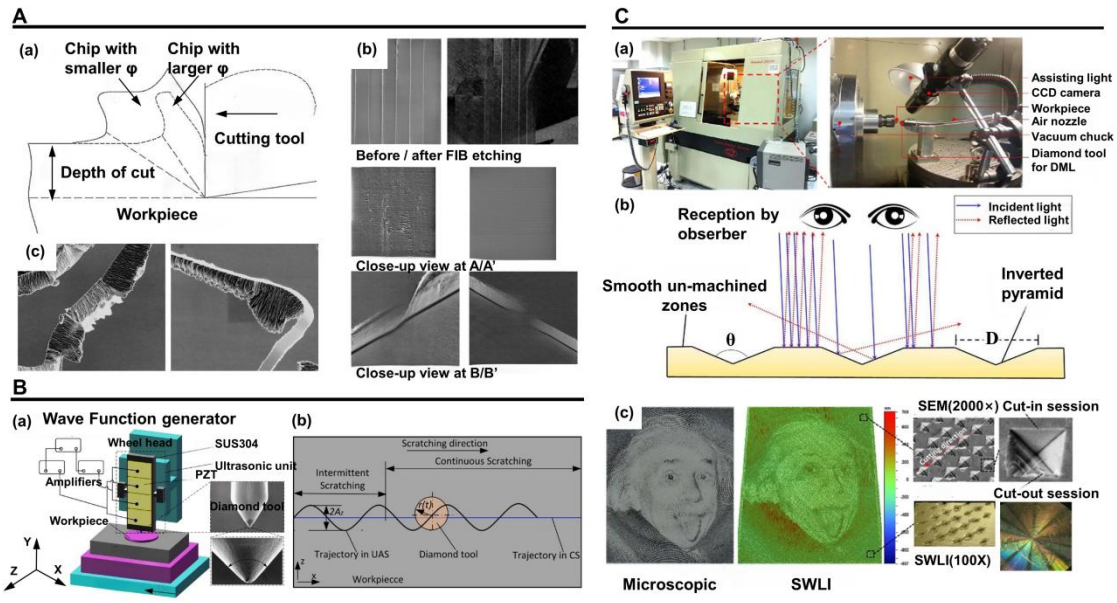

Fig. 3. SPDT techniques for fabricating structural-colour surfaces. (A) Cutting the surface with a height-to-depth ratio microcolumn array using single crystal diamond tools: (a) interaction between the chip and the cutting face for orthogonal cutting, (b) strategy to improve the machined surface and prevent burr formation, (c) chips generated with a reduced cross-feed of 1 m/pass.[32] Reprinted from[32], Copyright (2012), with permission from Elsevier. **(B)** Schematic diagram of ultrasonic-assisted processing: (a) schematic diagram of experimental setup, (b) schematic diagram of the tool path for ultrasonic-assisted scratch (UAS) trajectory.[34] Reprinted from[34], Copyright (2014), with permission from Elsevier. **(C)** Diamond micro-lithography (DML)

technique to transform grayscale images into pixelated microstructure arrays on metal surfaces: (a) experimental DML setup, (b) illustration of "bright" zone with unmachined surface and "dark" zone with inverted pyramids, and (c) finished surfaces characterized via microscopy, SWLI, SEM, and optical imaging.[37] Reprinted from[37], Copyright (2018), with permission from Elsevier.

Vibration-Assisted Machining

Vibration-assisted cutting (VAC) has emerged as a transformative structural colour engineering approach that enables precise micro/nanostructural control across diverse materials. By superimposing controlled vibrations onto conventional ultra-precision diamond cutting, VAC expands design flexibility and functional integration. Wang *et al.* [40] demonstrated this by using a precision vibration stage, as shown in **Fig. 4A(a)**, to create near-wavelength-scale gratings on acrylic polymers via controlled plastic deformation. The underlying mechanism, as illustrated in **Fig. 4A(c),** reveals how the diffraction-interference synergy converts geometric parameters into chromatic responses, achieving a remarkable 85% coverage of the visible spectrum with angular-dependent colour shifts, as shown in **Fig. 4A(b)**. These nanostructured surfaces demonstrate dual functionality as high-definition reflective displays and ultrasensitive refractive-index detectors.

Wang *et al.* [41] developed a flash-grating-based VAC system, as shown in **Fig. 4B(a)**, integrating ultrasonic vibration modules with multi-axis stages to achieve high-efficiency fabrication of structural colour graphics. This configuration enables synchronised tool oscillations that produce complex 3D grating profiles (period: 0.5-5 μm, minimum ~300 nm; blaze angle ~10°), as shown in **Fig. 4B(b)**, through controlled material deformation, which is particularly effective for polymers. Another typical work is shown in **Fig. 4B(c)**: embedded/orthogonal grating architectures (pixel size 50 μm×50 μm or 100 μm×100 μm) strategically designed to create optical variable devices (OVDs) exhibiting angle-dependent visual effects. Under different viewing conditions, these microstructured surfaces demonstrate programmable colour-image switching capabilities, as shown in **Fig. 4B(d)**, significantly advancing anti-counterfeiting technologies owing to their inherent optical security features.

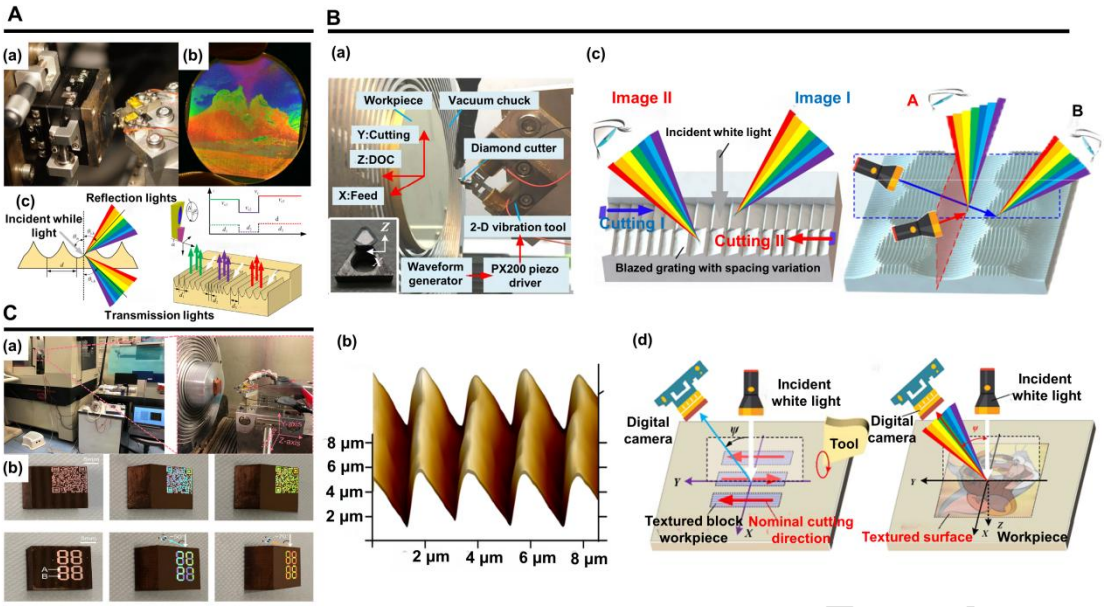

Fig. 4. Vibration-assisted cutting techniques for surface structural colour machining. (A) Vibration-assisted ultra-precision machining achieves structural coloration on non-metallic brittle surfaces: (a) hardware configuration, (b) structural coloration results on the surface of an acrylic polymer, (c) texturing principle [40]. Reproduced from Ref. [40], The Author(s), under the Creative Commons Attribution 4.0 International (CC BY 4.0) license. **(B)** Flash grating-based vibration-assisted diamond cutting enables rapid fabrication of structural colour graphics: (a) hardware configuration, (b) 3D grating profile, (c) OVD design for embedded/orthogonal gratings, (d) optical system for OVD appearance[41]. Reprinted from [41], Copyright (2022), with permission from Optica Publishing Group. **(C)** Novel 2DoF-VG for optical information control: (a) setup for generation/hiding, (b) demonstration of dynamic optical modulation [42]. Reprinted from[42], Copyright (2022), with permission from Elsevier.

Advancing toward multifunctionality, Du *et al.* [42] engineered a two-degree-of-freedom VAC system (2DoF-VG), as shown in **Fig. 4C(a)**, featuring synchronised multidirectional vibrations (maximal working frequency: 2200 Hz) and adaptive tool path control. This configuration enables concurrent fabrication of functional nanostructures (facet spacing: 585.9-677.0 nm) with dynamic optical modulation capabilities, as shown in **Fig. 4C(b)**. Through programmable adjustment of grating architecture across localised regions (pixel size: 70 μm × 70 μm), the platform achieves selective manipulation of light-matter interactions, allowing optical

characteristics to be strategically concealed or amplified.

Building on such programmable spatial control, another research direction leverages VAC for spectral engineering through surface topology optimisation. Wang et al.[43] developed a modulation-assisted ultraprecision machining variant of VAC, where a piezoelectric-actuated diamond tool generates controlled vibration trajectories (modulation frequency: 125 Hz) to fabricate multilevel submicron staircase profiles. The core principle involves optimising the surface structure to function as a wavelength-selective reflector via zeroth-order diffraction, where step heights determine the reflected wavelength, and the number of levels narrows the spectral bandwidth for high colour purity. This method offers nanometric accuracy and material versatility, yet faces challenges in terms of fabrication efficiency and angular stability.

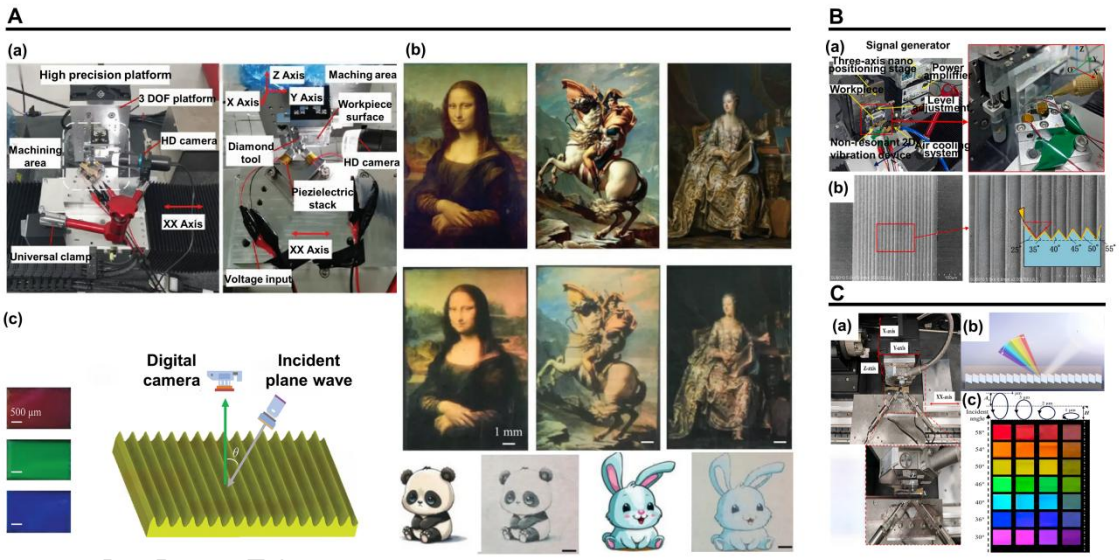

Fig. 5. Vibration-assisted cutting techniques for surface structural colour machining. (A) Multifrequency vibratory cutting (MFVC) fabricates optical Fourier surfaces for true structural coloration: (a) system (voltage generation and tool control), (b) diffraction-based patterned coloration, (c) colour effects via periodic gratings [44]. John Wiley & Sons. © 2023 Wiley Online Library. **(B)** Shape vibration cutting (SVC) creates relief gratings on hard-to-machine materials: (a) platform, (b) multi-blaze grating SEM morphology.[45] Reprinted from[45], Copyright (2023), with permission from Elsevier. **(C)** Vibration-assisted diamond cutting manipulates structural colour attributes: (a) nano-grating setup, (b) diffraction-induced colour mechanism, (c) elliptical

trajectory-based colour palette.[46] Reprinted from[46], Copyright (2024), with permission from Elsevier.

Furthermore, Ding *et al.* developed multifrequency vibratory cutting (MFVC), as shown in **Fig. 5A(a)**, to achieve frequency-domain structural colour control [44]. By superimposing tailored vibration profiles (frequency range: 200-1465 Hz) during machining, MFVC generates optical Fourier surfaces through engineered interference patterns, with spatial frequencies controllable up to 0.45 μm^{-1} and amplitude precision within 20 nm. This enables programmable diffraction and spatially resolved colour distributions, as illustrated in **Fig. 5A(b)**, with a maximum spatial frequency error of <5%.

A key advancement is RGB true-colour generation via subwavelength gratings (spacing: 455 nm-1.98 μm) utilising plasmonic and dispersive interactions, as shown in **Fig. 5A(c)**. The pixel size was 50 μm × 50 μm for a balance of resolution and efficiency, achieving a patterning rate of 0.2 mm^2/s. This method offers unparalleled spectral programmability for dynamic optical surfaces, but its reliance on multichannel synchronised control increases system complexity and cost.

Chen et al. established shape vibration cutting (SVC), as shown in **Fig. 5B(a)**, extending vibration-assisted fabrication to mid-infrared optics [45]. By combining kinematic toolpath planning with resonant vibrations (frequency: 36.5 kHz), SVC machines multi-blaze grating architectures (depth: up to 2.3 μm) on materials such as aluminium and silicon, as shown in **Fig. 5B(b),** enabling tailored light manipulation in the mid-IR range for applications in thermal management and molecular sensing. The primary advantage of SVC is its ability to process reflective and brittle materials for infrared applications, although it may face limitations in achieving high aspect ratios or fine feature sizes compared to processes dedicated to the visible spectrum.

Vibration-assisted diamond turning has evolved through kinematic trajectory engineering for structural colour control. Yang's foundational work [46] established a nanograting fabrication platform, as shown in **Fig. 5C(a)**, which combines

ultraprecision machining with resonant vibrations (frequency: 50 Hz) to deterministically program optical responses on metal surfaces. This method decodes microstructure–colour correlations via diffraction, with nanogratings featuring controllable spacing (400 nm-1000 nm) and height (30 nm-250 nm), thereby achieving full-spectrum colour rendering, as shown in **Fig. 5C(b)**. Its main strength is deterministic, high-fidelity fabrication of optical surfaces (spacing error <3.2%), although it is typically constrained to ductile materials and may require complex vibration tuning. Subsequent research by Lin and Yang demonstrated that transitioning from linear to elliptical vibration trajectories, as illustrated in **Fig. 5C(c)**, enhances the spectral purity by optimising the material removal process. Elliptical vibration improves surface quality and diffraction efficiency but can increase system complexity and pose challenges in maintaining consistent tool engagement over large areas.

Collectively, these advances demonstrate the versatility of VAC in tailoring structural colour properties, from static patterns to dynamic modulation, across industries ranging from security to optoelectronics. Future research should focus on scaling multi-material compatibility, integrating AI-driven process optimisation, and exploring hybrid systems for adaptive colour responses.

Elliptical Vibratory Cutting

Among the vibration-assisted cutting techniques reported, elliptical vibratory cutting (EVC) is increasingly valued for manufacturing structural colours. By superimposing elliptical vibrations during cutting, EVC enables the creation of periodic micro/nanostructures on surfaces. Suzuki et al. developed an EVC control system that actively modulates tool oscillation along the depth-of-cut direction, allowing dynamic depth control without a conventional fast tool servo [47]. As illustrated in **Fig. 6A**, the system integrates multi-axis platforms with piezoelectric actuators **(a)**, transfers the envelope of the elliptical vibration onto the workpiece to generate surface textures **(b)**, and achieves high-fidelity micro-engravings ranging from alphanumeric patterns **(c)**

to detailed colour motifs **(d)** on hardened steel.

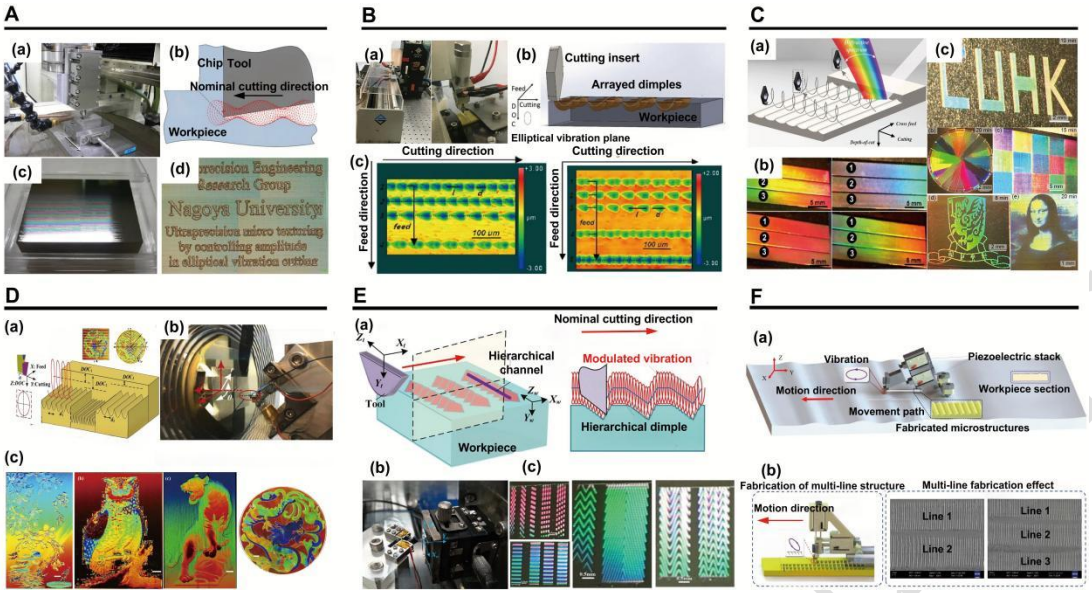

Fig. 6. Elliptical vibratory cutting techniques for surface structural colour machining. **(A)** Elliptical vibration texturing (EVT) for micro/nano engraving: (a) setup, (b) machining by controlling amplitude in elliptical vibration cutting, (c/d) sculptured letters (overview & close-up).[47] Reprinted from[47], Copyright (2011), with permission from Elsevier. **(B)** Micro-concavities via EVT are used for the rapid generation of flat engineering surfaces: (a) setup (X-Y-Z stage, actuator, adaptor), (b) schematic diagram of the EVT process, (c) textured profiles (Al 6061 & Brass C3600).[48] Reprinted from[48], Copyright (2023), with permission from Elsevier. **(C)** Periodic micro/nanostructures via parameter-tuned EVT: (a) ripple formation schematic, (b) iridescence via depth-of-cut variation, (c) pattern and image marking on brass surfaces.[49] Reprinted from[49], Copyright (2017), with permission from Elsevier. **(D)** Shallow relief carving combining engraving and EVT: (a) illustration of modulated elliptical vibration texturing, (b) modulated setup, (c) results of basso-relievo on brass samples. [50] Reprinted from[50], Copyright (2020), with permission from Elsevier. **(E)** Modulated EVT for microchannel fabrication: (a) proposed generation principle of hierarchical channels, (b) texturing setup, (c) optical image of generated hierarchical structures with iridescent effects.[51] Reprinted from[51], Copyright (2020), with permission from Elsevier. **(F)** Track-assisted robot for scalable microstructure fabrication: (a) robot working principle, (b) multiline mechanism [52]. Reproduced from Ref. [52], The Author(s), under the Creative Commons Attribution 4.0 International (CC BY 4.0) license.

Elliptical vibration texturing (EVT) has emerged as a transformative structural colouration technique that creates eco-friendly tunable colours through precisely engineered nanostructures, enabling scalable manufacturing across diverse substrates. Pioneering work by Yang *et al.* [48] established a high-speed EVT platform, as shown in **Fig. 6B(a)**, where ultrasonic elliptical vibration, driven by a trajectory modulation generator, produces discrete microdimples on metallic surfaces for light manipulation, as exemplified in **Fig. 6B(b)** on metallic substrates for broadband light manipulation. The processed surface is shown in **Fig. 6B(c)**. Through parametric modulation, graded nanoripples exhibits iridescence, as shown in **Fig. 6C(a)**, and interference-enhanced iridescence, as shown in **Figs. 6C(b) and 6C(c)**. This method allows dynamic optical tuning with submicron precision, but its effectiveness is constrained by the reflectivity and machinability of the workpiece material [53].

Subsequently, Wang *et al.* [49] developed EVT for functional surface engineering. The shallow relief carving system, shown in **Fig. 6D(a)**, synergises EVT with depth-graded control to simultaneously engrave topographic features and generate structural colour on the brass, as shown in **Fig. 6D(c).** This integration enables the creation of complex, optically active microstructures in a single process, although it increases the system complexity and demands precise synchronisation between texturing and engraving motions.

Furthermore, their modulated EVT platform, shown **Fig. 6E(b)**, redefines precision manufacturing through dual-mode fabrication capabilities[51] and employs a dual-mode tool vibration to fabricate hierarchical microchannels in a single step, as illustrated in **Fig. 6E(a)**. By alternating between vibration-assisted milling and diamond-turning kinematics, as shown in **Fig. 6E(c)**, surfaces are created where microchannels act as both optical elements and fluidic pathways. However, the need to optimise a large set of overlapping vibrations and kinematic parameters presents a significant challenge for process control and reproducibility.

Recent innovations in EVC methodologies have expanded their structural colour fabrication capabilities. Ding *et al*. [52] developed a portable EVC system

incorporating a piezoelectric microrobot, as shown in **Fig. 6F**; it generates surface microgrooves by combining elliptical vibrations with the autonomous locomotion of the robot, enabling the machining of curved surfaces. Concurrently, Li *et al.* [54] proposed an elliptical vibratory chiselling (EVC-chiselling) technique that employs backward-tool kinematics with superimposed vibrations to form ultrahigh-aspect-ratio microstructures from permanently deformed material chips.

Collective advances in vibration-assisted cutting (VAC) technologies have fundamentally expanded structural colour manufacturing capabilities, transcending conventional optical engineering limitations. This technological maturation enables transformative applications across three critical domains: advanced optical devices requiring programmable spectral responses, high-sensitivity biomolecular sensing platforms, and dynamic anticounterfeiting solutions with inherent security features.

Fly-Cutting Technology

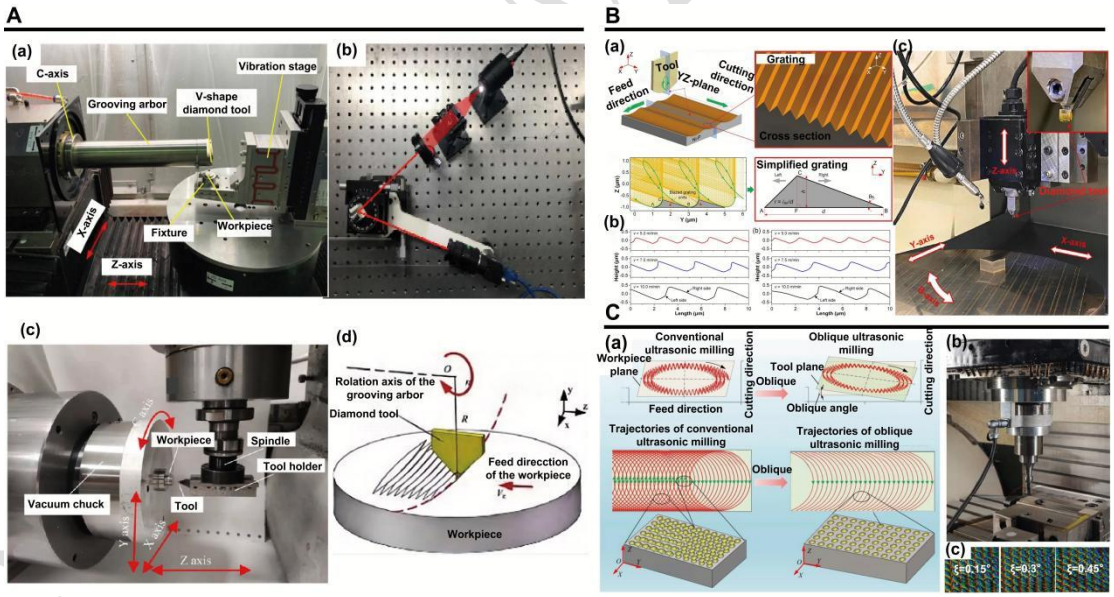

Fig. 7. Other processing methods for processing surface structural colours. (A) Processing of surface structural colours by fly-cutting processing technology.[55-57] Reprinted from[55], Copyright (2020), with permission from Elsevier. Reprinted from[56], Copyright (2020), with permission from Optica Publishing Group. Reprinted from[57], Copyright (2022), with permission from Elsevier. (a) AFC platform for structural-colour image manufacturing,

(b) colour spectrum detection experimental setup, (c) experimental setup for RFC, (d) schematic diagram of the AFC method. **(B)** UAUP processing method: (a) UAUP method for fabricating the blazed grating array, (b) cross-sectional profiles of the grating at different cutting speeds, (c) experimental setup of the UAUP method.[58] Reprinted from [58], Copyright (2023), with permission from Elsevier. **(C)** ORUM processing method: (a) Tool trajectories, (b) rotary ultrasonic milling experiment setup, (c) fabricated microstructures at different oblique angles on aluminium. [59] Reprinted from [59], Copyright (2023), with permission from Elsevier.

During the development of fly-cutting machining for structural colours, He *et al.* accomplished a significant advancement. Their axial feed fly-cutting (AFC) technique, illustrated in **Fig. 7A**, fabricates subwavelength grating structures that produce colour via optical diffraction and interference. This method has applications in optical filters, display technology, and anticounterfeiting. However, its capability is fundamentally constrained by limitations in generating intricate multiscale colour patterns, highlighting the need for advanced toolpath planning and precise spatial modulation.

To address these constraints, He *et al*. [55] pioneered vibration-assisted fly cutting (VAFC), which enabled the single-step fabrication of hierarchical micro/submicron structures on Ni-P substrates. The two-level architectures consist of first-order micro geometric features (period T_z:350-700 nm, line width ω_x:435-709μm, length l_z:348-701μm) and second-order submicron V-shaped grooves (period d: 200-800 nm, line width matching the period, aspect ratio ~1:2); this method offers efficient single-step hierarchical integration and flexible regulation of structural parameters, although it requires precise tuning of vibration parameters and feed rate to avoid tool-workpiece interference and ensure structural uniformity.

Subsequent refinement of the AFC methodology [60] achieved precise V-shaped submicron grooves (period: 100-1000 nm, line width matching period, aspect ratio ~1:2); this enables flexible period control via feed rate and high structural uniformity; however, the groove shape is limited to the tool profile, creating spectrally pure structural colours through controlled interference.

Subsequently, He et al. accurately fabricated submicron V-shaped grooves and structural colour patterns on Ni-P moulds using the newly developed AFC technique [56], with grooves featuring a period (spacing) of 200-1000 nm, line width matching the period, and an aspect ratio of ~1:2; this method leverages high cutting speeds and tool shape determinism for superior surface quality and uniform diffraction performance, although it requires strict spindle stability (dynamic balance P-V <10 nm) and groove tip removal to maintain structural precision.

In addition, He et al. proposed a VAFC-fabricated three-layer nanogroove structure [61] (1.2 mm, 30.2 μm, 300-800 nm periods; ~1:316, ~1:6, ~1:1 aspect ratios) that enhances specific wavelength diffraction via resonance for precise visible light control and array output, improving light utilisation but increasing process complexity with high positioning accuracy requirements.

Furthermore, He *et al.* [57] investigated the application of radial fly-cutting (RFC) technology for fabricating micro-structured surfaces, developing four modes, including the novel SA-HFRFC (for efficient complex hierarchical structures, **Fig. 7A(c))**; the microgrooves featured 0.1-10 μm period, 0.1-10 μm line width, ~1:1 aspect ratio, offering high cutting speed and structural precision, although stable spindle operation was required. This study introduced novel processing modalities/algorithms and experimentally validated their efficacy, opening new avenues for ultraprecision machining and deterministic fabrication of micro-hierarchical-structured surfaces.

Overall, fly-cut machining technology has undergone an evolution in structural colour fabrication from basic sub-micron trench fabrication to precisely controlled fabrication of complex microns and nanostructures. Each innovation in technology addresses specific technical challenges and introduces new properties and application prospects. The developmental trajectory, from AFC through VAFC to RFC, demonstrates continuous refinement in processing capabilities. These advancements have established a robust technological foundation for achieving high-resolution, high-contrast, and multicolour structural colour patterns while paving the way for

transformative approaches in next-generation optical device design and fabrication.

Ultrasonic Assisted Machining

In the field of structural colour fabrication, ultrasonic-assisted ultraprecision planarisation (UAUP) technology is an innovative processing method that creates colour patterns by fabricating gratings with serrated micro/nanostructures on high-phosphorus-electroplated Ni–P coatings. This approach takes advantage of the diffractive and reflective properties of these structures under light. Chen *et al.* [58] demonstrated that the UAUP technology has great potential for fabricating surfaces, specifically those exhibiting optical functions, as shown in **Fig. 7B,** which not only precisely control the propagation path of light but also produce rich colou Overall, fly-cut machining r effects. This technology offers ultra-high efficiency (41,400 units/s) and precise control (<5.25% constant error). However, it is sensitive to cutting speed/amplitude, enabling applications in optical communication and structural colouration.

Oblique rotational ultrasonic milling (ORUM) is an innovation structural colour manufacturing technology proposed by Zheng *et al.* [59] for the precise fabrication of micrometer-scale structures on aluminium and titanium alloys surfaces, as shown in **Fig. 7C**. Its operational principle involves tilting the tool rotational axis (0.15°-0.45°) and integrating longitudinal-torsional coupled ultrasonic vibration (19.5 kHz frequency, 8-12 μm amplitude) with tool rotation and feed motion to eliminate secondary recutting interference in conventional rotary ultrasonic milling for regular tool trajectories along the feed direction. Its advantages are high microstructure geometric regularity, flexible parameter tunability, and adaptability to freeform surfaces, while its drawbacks include reliance on precise multi-parameter control and increased initial setup costs resulting from specialised equipment and tool requirements.

Collectively, UAUP and ORUM exemplify the transformative potential of ultrasonic vibration-based machining in structural colour fabrication, driving innovation across

industries and paving the way for intelligent, durable, and environmentally friendly colour solutions.

In summary, different mechanical processing technologies possess distinct characteristics and have developed distinct performance differentiation advantages (see **Table 1**). Together, they drive the evolution of structural colour manufacturing from single-function applications to high precision, multifunctionality, and large-scale production.

Table 1 Quantitative comparison of five structural colour machining methods

Comparison Dimension	SPDT	VAM	EVC	FCT	UAM
Machining Principle	Periodic microstructure formation via tool-workpiece relative motion.	microstructure period controlled by vibration trajectory	Elliptical tool vibration cutting periodic ripples/gratings for light diffraction	High-speed rotating diamond tool synchronized with the workpiece feed; one groove per rotation	Ultrasonic vibration+ milling/planning; ORUM tilts tool axis to avoid secondary cutting
Precision	Dimensional error <5%, Ra <10nm	Period deviation <3%, Ra <50nm	Grating spacing accuracy ±3nm, Ra <100nm	Period deviation <5%, Ra <10nm, groove parallelism error <2%	Grating constant error <5.25%/ microstructure regularity >90%, Ra <100nm
Scalability	Planar/simple curved surfaces	Scalable to hierarchical structures	Large-area; multi-DOF system compatible	Large-area (≤20mm×20mm) & freeform surfaces	Area ≤20mm×20mm
Durability	Service life >5 years	Stability depends on vibration parameters	Optical performance retention >8 years	Ni-P mould reusable >100 times	Stable long-term grating diffraction performance
Optimal Application Scenarios	Simple periodic microstructures, high-precision optical substrates	Structural colour patterns, microfluidic chip surfaces, low-friction functional surfaces	Anti-counterfeiting marks, metal decorative surfaces, optically variable devices (OVDs)	High-precision gratings, structural colour image reproduction, glass moulding tools	Sawtooth gratings, freeform functional surfaces (implants/wings), anti-counterfeiting marks
Resolution	Pixel size ≥50μm×50μm	Pixel size ≥40μm×40μm	Pixel size 20μm×20μm-100μm×100μm	Pixel size 85.4μm×85.4μm-1mm×1mm	Microstructure spacing tunable to submicron scale

Speed	Machining rate 0.1–0.5mm²/s	Machining rate 0.2–0.4mm²/s	Vibration frequency 28–41.4kHz	Spindle speed 3000-10,000rpm; machining rate 0.2–0.4mm²/s	41,400 grating units/s; spindle speed 3000–8000rpm
Materials Used	Copper, aluminium, Ni-P coating, optical plastics	Aluminium, stainless steel, Ti6Al4V, Ni-P coating	Brass, Al 6061, stainless steel, copper, hardened steel (HRC53)	Ni-P coating, aluminium, titanium alloy, stainless steel	Ni-P coating/ aluminium alloy, Ti6Al4V, stainless steel
Cost	Medium equipment investment; high tool cost	Medium-high equipment investment	High equipment investment	High equipment investment	High equipment investment

Non-Mechanical Processing

Lithography Processing

The evolution of photolithography in structural colour manufacturing has traced a trajectory from fundamental research to transformative applications. The precise control of light exposure and development enables complex micron-to-nanometre patterns, with the core devices and working principles detailed in **Fig. 8A** and **Fig. 8B**. Back in 2012, Han *et al.* [62] employed optofluidic maskless lithography to fabricate QR-coded polymer micro-labels (10-50 μm module widths), enhancing drug authentication reliability and combating counterfeiting. However, this method is inherently constrained to planar structures, precluding 3D structural colours with trade-offs such as micron-scale resolution (limited by UV diffraction), scalability challenges from microfluidic channel constraints, and higher costs due to specialised equipment, restricting its broader utility.

Building on this, Chen *et al* [63] proposed Dip-pen nanodisplacement lithography (DNL), a scanning probe lithography-based technique enabling large-area (1 cm^2) patterning of metallic nanostructures with sub-100 nm resolution (minimum feature size 70 nm) and ≤10% uniformity. By tuning the feature densities, pattern designs, and key parameters (z-extension and dwell time), DNL fabricates complex 2D/3D architectures that modulate optical properties such as plasmon resonance (centred at ~640 nm for nanorods). However, DNL faces inherent trade-offs: its resolution is

limited by the Au grain size (~30-50 nm) and tip apex curvature (~60 nm); scalability beyond cm² areas is constrained by tip array uniformity; and current tip arrays only replicate identical patterns, hindering customisation for increasingly complex 3D architectures.

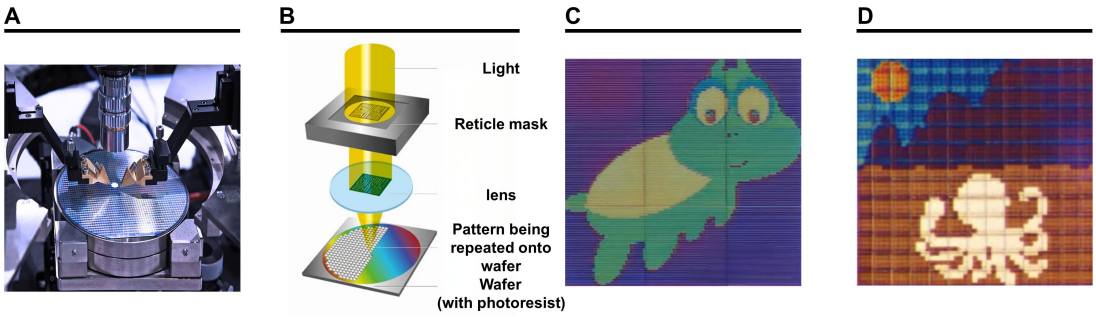

Fig. 8. Photolithography processing technology for surface structure colour. (A) Photolithography experimental setup. **(B)** Photolithography processing schematic. **(C)** Colourful turtle pattern processed by TPL.[64] John Wiley & Sons. © 2022 The Authors. Advanced Materials published by Wiley-VCH GmbH. **(D)** Colourful octopus pattern processed by TPL.[65] Reprinted from [65], Copyright (2021), with permission from Springer Nature.

Advancing beyond these limitations, Zhang *et al.* [66] utilised two-photon polymerisation lithography (TPL) to fabricate submicron grid structures (300 nm half-pitch, 280 nm linewidth) from shape memory polymers (SMPs), enabling size-tunable multicoloured patterns via geometric parameter control (height: 0.9-2.7 μm, pitch: 2 μm). This technique, which achieves shape memory effects through nanoscale deformation flattening, renders colourless structures for information hiding. Heating above the glass transition temperature (≈ 80 °C) recovers the original topography and colours within seconds offering unique visual variability for anti-counterfeiting. However, this technique also faces trade-offs: high-resolution patterning (≈21150 dpi) is offset by low throughput (2 h/cm^2) and high costs due to serial writing of the TPL, which limits large-scale production.

Huang *et al.* [67] developed patterned pulse laser lithography (PPLL), a highly efficient technique for large-area (10×10 mm^2) nanoscale patterning on thin-film substrates (metals and GST) under ambient conditions. By using ultrafast laser pulses with

gradient-boundary quasi-binary phase masks and circular polarisation, PPLL weakens diffraction and polarisation asymmetry, achieving sub-wavelength resolution (303 nm feature size) and uniform periodic structures (period: 0.45-15 μm) with a throughput of 250,000 concentric rings in 5 minutes. Its strength lies in the scalable fabrication of homogeneous metasurfaces; however, it lacks precise control over fine 3D features, as one-step ablation/modification limits the structural complexity compared to TPL.

Complementary to PPLL, Chan *et al.* [68] achieved full geometric control of hidden colour information in diffraction gratings via TPL, encoding up to five sets of data (potentially 18) by tuning height (0.6-1.8 μm), periodicity (0.8-1.6 μm), and orientation. The technique simplifies illumination to a single white light source (no waveguides required) and suppresses crosstalk via ≥10° angular separation between grating sectors, enabling angular multiplexing for security watermarks. However, it is constrained by grating structural diversity and relies on the low throughput of the TPL, restricting applications requiring complex 3D architectures.

Concurrently, Zhang *et al.* [65] employed two-photon polymerisation lithography (TPL) to fabricate submicron grid structures (rather than nanopillars) with a 300 nm half-pitch resolution and tunable linewidth (280-630 nm) and height (0.98-1.99 μm) from a Vero Clear-derived shape memory polymer (SMP). Externally stimulated by heat (80 °C) and stress (~500 kPa), these structures flatten to a colourless state and recover rapidly to generate high-resolution (≈21150 dpi) reconfigurable structural colour prints, as illustrated in **Figs. 8C** and **8D**. While promising for optical patterning, the technique faces inherent trade-offs: serial writing of the TPL limits scalability (2 h/cm^2 throughput) and raises costs, and its resolution (~300 nm half-pitch) lags behind commercial photoresists (~100 nm), with durability constrained to ≤10 programming cycles before edge collapse.

Collectively, lithography has evolved into structural colour fabrication, from planar pattern fabrication to 3D structure creation, to precisely control optical effects. Each technological breakthrough has concurrently introduced novel functionalities while overcoming domain-specific limitations, thereby propelling photolithography beyond

conventional manufacturing paradigms. As this evolution continues, next-generation lithographic approaches promise to unlock unprecedented capabilities in structural colour engineering and precision photonic device fabrication.

Laser Processing

In the field of structural colour fabrication, laser processing technology has spurred innovative methods to expand fabrication capabilities and applications. Rubahn K *et al.* [69] used 193 nm UV lasers to induce grating structures (1 μm period, ~6 nm height, 500 nm ridge width) on Polydimethylsiloxane (PDMS) thin films, achieving effective diffraction with minimal corrugation. These authors demonstrated the potential of UV lasers for micro/nanostructuring. However, this technique faces trade-offs: a low aspect ratio (~1:167) limits structural complexity, and the rubbery state of PDMS causes lateral flow, restricting resolution and scalability.

Liu *et al.* [70] summarised three femtosecond laser colouration mechanisms for solid substrates: surface oxidation, laser-induced periodic surface structures (LIPSSs), and surface plasmon resonance (SPR) of metallic nanostructures. These mechanisms modify the surface optical properties to produce visible colours, with microgrooves (**Fig. 9A**) enabling specific optical functions via laser engraving. However, oxidation-based colouring lacks colour completeness, LIPSSs (540 nm period) are angle-dependent, and SPR relies on expensive femtosecond lasers, which limits the cost-effectiveness of large-scale production.

Vorobyev and Guo [71] used femtosecond laser pulses (800 nm, 65 fs) and tuning parameters to turn Al golden via nanostructuring and NC-LIPSSs. Spectroscopic measurements confirmed controllable optical property alteration, but the technique suffers from low productivity (0.005-0.8 mm^2/s for LIPSSs), high equipment costs, and poor colour stability.

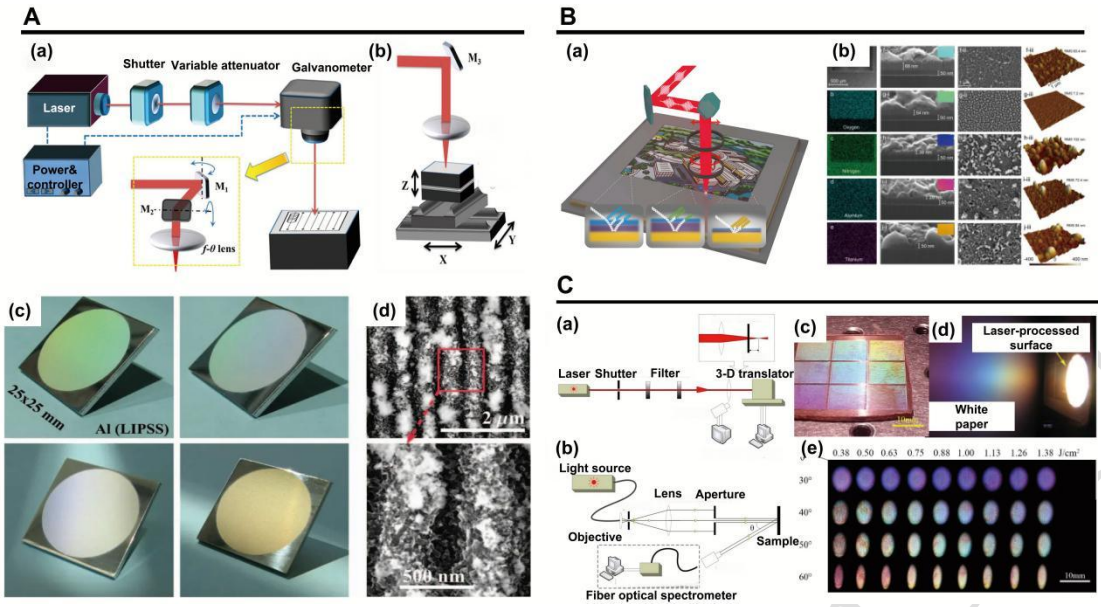

Fig. 9. Laser processing technology for surface structure colour. (A) Experimental setups for laser colour marking: (a) galvanometer scanning; (b) translation stages. M1, M2, and M3 denote mirrors; (c) angle-dependent colour appearance, (d) SEM images of NCLIPSSs on the sample.[70] Reprinted from [70], Copyright (2019), with permission from APL. **(B)** Method for obtaining structural colour through ultrashort pulse laser: (a) schematic of surface colouring using ultrafast lasers, (b) SEM image and corresponding EDX maps of a laser-written area with green colour.[72] Reprinted from [72], Copyright (2023), with permission from Springer Nature. **(C)** Colour features of laser-treated copper: (a) setup for the out-of-focus laser processing technique; (b) setup for the optical and spectral characterizations of the laser processing sample surface**,** (c) multicoloured appearance under white light; (d) grating rainbow projection; (e) colour evolution with laser fluence and viewing angle[73]. Reprinted from [73], Copyright (2020), with permission from Optica Publishing Group.

Advancing femtosecond laser applications, Ou *et al.* [73] developed an "out-of-focus processing method" to create near-subwavelength ripples (500-667 nm period) on pure copper surfaces, achieving angle-dependent colorization via grating diffraction, as shown in **Fig. 9C**. This non-contact approach offers flexibility for label marking but faces trade-offs: low laser fluence (<0.75 J/cm^2) leads to incomplete ripple coverage and diffuse reflection interference, while high fluence (>1.13 J/cm^2) saturates period tuning, limiting colour diversity. This technique also requires

expensive femtosecond lasers, which hinder cost-effective scalability.

Nauval *et al.* [74] proposed a visible femtosecond laser-based 4f imaging system to characterise thin-film magnetic properties by observing the diffraction and interference patterns by varying the object plane apertures. This provides a new tool for structural colour analysis; however, it is limited to numerical simulations and low resolution, restricting its use for subwavelength feature characterisation.

Concurrently, Fantova *et al.* [75] realised single-step fabrication of tunable blazed gratings on stainless steel using triangular femtosecond pulses, thereby generating asymmetric grooves (asymmetry ratio up to 5) by adjusting the processing direction. This alternative to conventional methods enables flexible sidewall angle control but suffers from low throughput (3-10 mm/s scanning speed), high equipment cost, and lateral beam overlap issues that reduce grating homogeneity for large-area fabrication.

Direct Laser Writing (DLW) is an advanced maskless fabrication technique that enables direct micro/nanoscale patterning via precise laser-material interactions, eliminating traditional lithographic masks for flexible surface structuring. In a recent breakthrough, Mu *et al.* [76] used DLW to synthesise laser-induced graphene (LIG) directly on biomass-derived liquid carbon precursors through photothermal reactions, achieving substrate-specific patterning with micron-scale accuracy by modulating the laser power (3 W), scan velocity (0.27 m/s), and pixel density (1000 PPI). This approach opens new pathways for flexible electronics, particularly wearable biosensors and energy devices, but faces inherent trade-offs: low throughput (slow scan speeds) limits large-scale scalability, while its resolution (minimum LIG line width ~90 μm) is coarser than lithography, restricting high-precision microelectronics use.

The development of laser processing technology in structural colour manufacturing reflects the evolution from single-ultraviolet (UV) laser grating formation to femtosecond laser pulsed colouring to highly tunable grating manufacturing based on ultrashort pulsed lasers and DLW technology. **Table 2** presents a quantitative

comparison of structural colour fabrication via lithography and laser processing. The development of these technologies not only improves the precision and efficiency of structural colour fabrication but also broadens the prospects of its application in the fields of optics, display technology, and anti-counterfeit marking[77]. With the continuous progress of laser processing technology, we expect it to play a more critical role in the future of structural colour fabrication and precision engineering and to bring more innovations and breakthroughs in the design and fabrication of optical devices.

Table 2 Quantitative comparison of photolithography and laser processing

Fabrication Category	**Lithography Processing**		**Laser Processing**		
Processing Method	**TPL**	**NIL**	**Femtosecond Laser Colouring**	**RLP**	**DLW**
Working Principle	Femtosecond laser-induced photopolymerization of photoresist to form 3D micro/nanostructures	Pattern transfer from mould to resist via thermal/UV curing	Laser-induced oxidation, LIPSS formation, or SPR via metallic nanostructures	Photothermal remodelling-induced resonance for colour control	Photothermal reaction for in-situ synthesis of patterned LIG
Optimal Application Scenarios	High-resolution 3D photonic crystals, microactuators, autostereoscopic displays	Large-scale plasmonic colour printing, microfluidic chips	Metal decoration, anti-counterfeiting marks, wearable device colouring	High-resolution full-colour printing, optical data storage	Flexible biosensors, wearable electronics
Resolution	Submicron (1.45 μm voxel)	Submicron (100 nm feature)	Nanoscale (400 nm LIPSS)	Ultra-high (100,000 dpi)	Micron (90 μm linewidth)
Processing Speed	Low (5000-10000 μm/s writing speed)	High (roll-to-roll compatible)	Low-Medium (0.005-60 mm^2/s)	Medium (10 cm^2/s throughput)	Low (0.27 m/s scanning speed)
Materials Used	Acrylate-based photoresist, CLC monomer mixture	Polycarbonate, photoresist, mould materials	Al, Cu, Ti, stainless steel, Si	Ge, PMMA, TiAlN-TiN hybrid films	Biomass-derived liquid carbon precursors, PDMS
Cost Level	High	Medium	High	High	Medium

Scalability	Poor (slow throughput)	Strong (batch production)	Strong (large-area)	Medium (2D patterns)	Medium (flexible substrates)
Durability	High (heat/humidity stable)	Medium (resist-dependent)	High (wear/corrosion-resistant)	High (UV/salt fog-resistant)	High (10,000 cycles stable)
Precision Control	Lattice constant ±10 nm	Pattern replication ±20 nm	LIPSS period ±10 nm	Nanopore diameter ±5 nm	Pattern geometry ±10 μm

Other Approaches

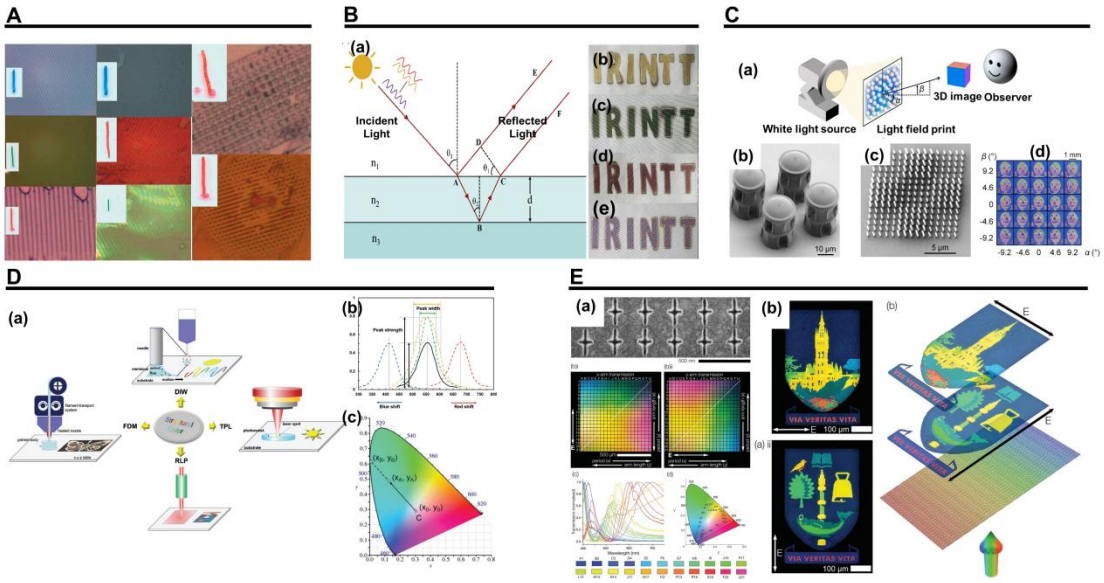

Fig. 10. Other processing methods for structural colour. (A) Patterns via polycarbonate and Al foil moulds on OHP film and glass. [78] Reprinted from [78], Copyright (2001), with permission from American Chemical Society. **(B)** Fabric structural colouring by magnetron sputtering of bilayer films on polyester.[79] Reprinted from [79], Copyright (2020), with permission from Elsevier. (a) Interference mechanism; (b-e) "IRINTT" pattern with various colours. **(C)** Structured colour printing with microlens arrays.[80] Reprinted from [80], Copyright (2022), with permission from Elsevier. (a) Light-harvesting principle; (b) 2×2 display units SEM; (c) 3×3 pixels SEM; (d) 5×5 cartoon face viewpoints. (**D**) Combination of 3D printing technology and structural colour materials.[81] John Wiley & Sons. © 2023 The Authors. Advanced Material Technologies published by Wiley-VCH GmbH. (a) Design and application of structural colour materials by different 3D printing methods; (b) schematic of spectral

reflectance; (c) CIE chromaticity space. (**E**) New technology for achieving high-density image coding by using plasma colour filters.[82] John Wiley & Sons. © 2023 The Authors. Advanced Functional Materials published by Wiley-VCH GmbH. (a) Nanopixel properties; (b) Switchable characteristic of the information displayed by a single group of nanopixels.

Beyond laser processing and photolithography, diverse nonmechanical structural colour fabrication methods rely on alternative physical principles, as shown in **Fig. 10**. Key approaches include printing technologies and plasmonic resonance engineering where metallic nanostructures manipulate light via localized surface plasmon oscillations to generate tunable structural colours with foundational work conducted by Knop *et al.* [83] in 1978. Knop's transmission phase gratings featured deep rectangular grooves in transparent media, with grating constants $d = \lambda$ to 5λ, linewidths bd (aspect ratio b=0.3 for optimal performance), and depths $a<5\lambda$. This method uses diffraction-based colour filters for microformat image storage, establishing core subwavelength optical manipulation principles; however, its resolution is constrained by groove geometry, scalability is limited by specialised fabrication, and cost is elevated owing to precision etching requirements.

Subsequently, Schueller *et al.* [84] introduced reconfigurable microfluidic diffraction gratings in 1998, comprising PDMS elastomers and glass substrates with microchannels (width: 50 μm, depth: 20 μm, period: 100 μm). By filling channels with fluids featuring varying refractive indices and optical densities, they generated light phase differences and amplitude changes to drive diffraction, enabling dynamic tunability with low material costs; however, switching times (50-500 ms) are slower than electrostatic alternatives, scalability is hindered by microchannel fabrication complexity, and resolution is limited to micron-scale features.

Contemporary advances have further democratised fabrication. Chowdhury *et al.* [78] developed a facile approach in 2001 using commercial permanent markers to draw lines on OHP paper/glass, then transferring CD-derived patterns (line width: 0.8 μm, depth: 0.5 μm, period: 1.6 μm) onto these lines, as shown in **Fig. 10A**. This low-cost, accessible method enables submicron colour patterns and cross-structures via

perpendicular imprinting; however, manual operation limits large-scale reproducibility, and the resolution is capped by the inherent structural constraints of the CD mould.

A consistent trade-off emerges across these methods: cost reduction and accessibility often sacrifice resolution or scalability, whereas high-resolution approaches demand specialised fabrication or materials, highlighting the need for application-specific trade-off prioritisation.

Furthermore, Görrn and Wagner [85] established the fundamental link between surface wrinkling and structural colouration via plasma-enhanced oxidation of PDMS, creating a stiffened surface layer (10.1-114.3 nm thick) with a graded elastic modulus (47.7-3240.9×substrate modulus) that drives spontaneous wrinkling into periodic architectures (wavelength: 250 nm-2.25 μm, amplitude: 340-1280 nm, aspect ratio ~0.01-0.5). This strain-induced self-assembly generates colour through light interference, offering large-area scalability and low cost but also limited resolution control and sensitivity to plasma parameters (pressure/dose), which can cause cracking.

Wu *et al.* [86] explored two-stage wrinkling in magnetron-sputtered Al films on PDMS, achieving hierarchical nanostructures: nanoscale wrinkles (wavelength ~200 nm, amplitude ~40 nm, aspect ratio 0.2) and micro-scale wrinkles (wavelength 1.3-9.2 μm, amplitude 45-400 nm, aspect ratio 0.005-0.04) tuned by film thickness (20-100 nm) and deposition temperature (25-180 °C). This method enables programmable optical interference with facile fabrication but trades off uniformity for hierarchical complexity, with scalability constrained by substrate thermal stability.

Zhang *et al.* [79] translated these principles into textiles via silver/silver oxide bilayer deposition on polyester fibres, as shown in **Fig. 10B**. Precise oxide thickness control enables wavelength-selective interference across the visible spectrum, creating durable structural colouration. **Fig. 10B(a)** illustrates the interference mechanism, while panels in **Fig. 10B(b)-(e)** demonstrate complex “IRINTT” patterning, achieving large-area, high-resolution colouration on flexible substrates, but suffering from poor

washing fastness and limited resolution due to fibre surface roughness, balancing functional integration with practical durability trade-offs.

Kumar *et al.* [87] developed a non-pigment colour printing method that leverages plasmon resonance in metal nanostructures (Ag/Au nanodisks: diameter 50-140 nm, gap 30-120 nm, periodicity 120-250 nm, aspect ratio ~0.36-2.8), enabling 100,000 dpi resolution at the optical diffraction limit. Fabricated via electron-beam lithography (EBL) and scalable nanoimprint lithography (NIL), this technique encodes colour through tunable plasmon/Fano resonances for sharp chromatic transitions and subtle tonal gradations, but suffers from high initial EBL costs and a limited colour gamut compared to pigment methods.

Chan *et al.* [80] integrated structural colour printing (SCP) with microlens arrays (MLA) for sustainable autostereoscopic displays. The SCP features nanopillars (300 nm diameter, 1.3-1.9 μm height, aspect ratio ~4.3-6.3, periodicity 50 μm) were fabricated via two-photon polymerisation (TPL), while MLAs (diameter 21 μm, radius of curvature 22 μm, focal length 37 μm) were made via photolithography/thermal reflow or TPL. As shown in **Fig. 9C(a)**, this synergy generates naked-eye 3D visualisation under white light (**Fig. 9C(d)**) without external optics, offering low power consumption and recyclability (polymer dissolution in organic solvents); however, the slow throughput of the TPL limits large-scale production.

Collectively, these innovations demonstrate printed structural colours for high-resolution multichromatic patterning with exceptional contrast. **Table 3** presents a quantitative comparison of structural colour fabrication using other non-mechanical approaches. They have opened transformative pathways for advanced optical device manufacturing, as shown in **Fig. 10D** [81].

Table 3 Quantitative Comparison of other approaches

Processing Method	Diffraction Gratings (Knop)	Microfluidic Gratings	Surface Wrinkling (Plasma/Sputtering)	Thin-Film Interference (Ag/Ag_2O)	Plasmonic Resonance (Ag/Au Nanodisks)	CD Template Imprinting

Working Principle	Light diffraction by deep rectangular grooves in transparent media	Phase/amplitude modulation via fluids with varying refractive indices/optical densities	Stress-induced periodic wrinkling of stiffened surface layer	Wavelength-selective interference of reflected light from bilayer films	Localized surface plasmon/Fano resonance in metallic nanostructures	Pattern transfer from CD's periodic structures via pressure
Optimal Application Scenarios	Micro-format image storage, diffraction-based colour filters	Dynamic optical filters, microfluidic sensors	Large-area flexible optical films, anti-reflective surfaces	Textile waterless dyeing, smart wearable decoration	Ultra-high-resolution security marks, nanoscale colour filters	Low-cost submicron patterning, educational demonstrations
Resolution	Submicron (λ-5λ period)	Micron (50 μm channel)	Nano-micron (250 nm-9.2 μm)	Micron (film thickness ±2 nm)	Nanoscale (250 nm pixel)	Submicron (0.8 μm linewidth)
Processing Speed	Low (precision etching)	Low (50-500 ms switching)	Medium (plasma/sputtering <2h)	Medium (sputtering <1h)	Low (EBL writing <10h/wafer)	Medium (single imprint <1min)
Materials Used	Transparent dielectric, glass	PDMS, glass, NaCl/KSCN solutions, dyes	PDMS, polyimide, Al films	Polyester fabric, Ag, Ag_2O	Ag/Au nano disks, HSQ resist, Si substrate	OHP paper, glass, CD polycarbonate/aluminium foil
Cost Level	High	Medium	Low-Medium	Medium	High	Low
Scalability	Poor (single-piece etching)	Poor (microchannel complexity)	Strong (large-area uniform)	Strong (fabric large-area)	Medium (NIL scalable)	Medium (manual operation-limited)
Durability	Medium (≤150°C stable)	Medium (chemical-resistant)	Medium (crack-prone)	Low (poor washing fastness)	Medium (Au-protected)	Low (ink wear-prone)
Precision Control	Groove width/period ±5%	Channel size ±2 μm	Wrinkle period ±10 nm	Oxide layer thickness ±2 nm	Nano disk size ±3 nm	Pattern replication ±0.1 μm

The evolution of nonmechanical structural colour fabrication reveals a multifaceted technological trajectory, progressing from classical diffraction gratings to

contemporary nanophotonic engineering [88-91]. From early grating techniques to modern methods based on microfluidic and plasma processing, advanced laser direct writing techniques, and nanostructure manipulation, these innovations have continually redefined manufacturing boundaries, enhancing both spatial resolution and dynamic control, while enabling transformative applications, such as ultrahigh-resolution displays, unforgeable optical security features, biophotonic sensors, and multidimensional optical data storage. The convergence of photonics, materials science, and nanofabrication promises next-generation structural colour platforms with unprecedented functional integration, as shown in **Fig. 10E** [82].

Dynamically Tunable Structural Colours

Dynamic structural colour generation enables real-time modulation of photonic responses through stimuli-responsive reconfiguration of surface micro/nanoarchitectures via mechanical, thermal, or optical actuation [92-96] This paradigm facilitates programmable colour transitions with subwavelength precision, meeting critical demands across intelligent displays, wearable photonics, unforgeable security systems, and real-time biomedical diagnostic interfaces. Over the past two decades, there have been transformative advances, particularly in microfluidic monitoring platforms, stimuli-active material development, nanolithographic fabrication, and field-integrated applications. These innovations not only establish new benchmarks for dynamic structural colour performance but also create foundational platforms for next-generation adaptive photonic systems.

Microfluidic Monitoring and Pressure Sensing

Innovative approaches to real-time pressure monitoring in microfluidic devices leverage deformable diffraction gratings and PDMS-based replication techniques to achieve dynamic optical control. The deformable diffraction grating method utilises PDMS grating structures, where pressure-induced deformations alter the diffraction efficiency, enabling noninvasive detection of localised fluid pressure. This strain-mediated response relies on the reversible, linear-elastic deformation of PDMS

within ~8% strain, offering good short-term reproducibility, as demonstrated in controlled cyclic pressure tests. Fabrication involves deep reactive ion etching (DRIE) of patterned gratings on silicon wafers, followed by SU-8 photoresist-defined microchannels and PDMS replication, ensuring cost-effective and high-sensitivity monitoring [97].

However, the long-term stability and environmental robustness of such PDMS-based gratings require further investigation because factors such as temperature variations, humidity, and material aging may affect the Young's modulus of PDMS and the adhesion at the PDMS-glass interface, potentially drifting the pressure-optical response over time. Complementary PDMS replication mould technology creates pressure-responsive devices using soft lithography. Internal pressure changes dynamically modulate the grating colour and beam intensity through structural adjustments, demonstrating precise optical property control. The reproducibility of this optical response across devices depends critically on the consistency of the fabrication parameters, including PDMS curing, grating geometry, and bonding quality. This approach extends beyond microfluidics to applications such as fibre-optic pressure sensing, and highlights its versatility [98].

Both methods exploit the flexibility and optical tunability of PDMS, establishing foundational strategies for real-time adaptive sensing in biomedical and fluidic systems; however, their adoption in varying environmental conditions calls for enhanced material stabilisation and packaging strategies to ensure reliable operation.

Flexible Materials and Composite Architectures

Advanced flexible composites enable unprecedented dynamic optical control via engineered mechano-optical responses. A stretchable transparent heater composed of silver nanowires (Ag NWs) embedded in PDMS films demonstrates dual functionality, providing real-time thermal management for wearable electronics while maintaining optical transparency, which is ideal for personalised healthcare applications [99]. The

system exhibits stable operation up to 60 °C under 60 % tensile strain, with reproducible thermal response over repeated stretching cycles. Partial embedding of the Ag NW network in PDMS improves the interfacial adhesion and suppresses the resistance drift during cycling, enabling reliable Joule heating. Voltage adjustment can compensate for strain-induced resistance variations to maintain a steady temperature. However, the long-term reliability of durable wearable devices under combined thermomechanical cycling and environmental exposure requires further investigation.

Tunable organic/inorganic composite one-dimensional photonic crystals (1D-PCs) exhibit strain-responsive colour shifts in the visible spectrum. By applying mechanical strain, these elastic 1D-PCs reversibly modulate the photonic band gaps, serving as high-sensitivity optical strain sensors for smart material systems, as shown in **Fig. 11A(a)**, where digital photos of the 6-layer 1DPC can be observed. These photos display distinct colour shifts from red at 0% strain to blue at 40% strain [100]. These sensors exhibit good cyclic durability over 100 stretching cycles with repeatable sensitivity (~3.9 nm/%), though a gradual decrease from an initial -6.05 nm/% indicates material aging under prolonged strain. Their stability under varying environmental conditions requires further investigation for reliable real-world applications.

Further enhancing adaptability, a PDMS/SiO_2 nanoparticle composite laminate dynamically transitions between transparent and coloured states under mechanical stress, leveraging the contrast between soft PDMS and rigid SiO_2 phases. This mechanochromic response is achieved through strain-mediated reconstruction of the embedded diffraction grating, which reversibly tunes the photonic bandgap. The system demonstrates significant stability under varying temperatures (20-70 °C) and during repeated mechanical cycling, attributable to the robust PDMS/SiO_2 interface and the elastic recovery of the matrix. It also shows high reproducibility over extended cycles with minimal hysteresis and degradation in colour contrast, and offers novel solutions for anti-counterfeiting and interactive displays, as shown in **Fig. 11A(c);** this figure depicts the colour-change process of this strain sensor under tensile conditions [101-103].

Complementing these, a ZnO/ZnF_2 heterostructure achieves dynamic surface pattern regulation via stress-triggered mechanical photoluminescence. External mechanical loads induce localised lattice distortions, generating tunable photoluminescent emission for real-time colour or pattern modulation. The system exhibits notable stability and repeatability under cyclic mechanical loading owing to the robust heterojunction interface and the elastic recovery of the PDMS matrix, which jointly ensure consistent stimulus–response behaviour across varying environmental conditions, as shown in **Fig. 12A(c).** This figure refers to the anticounterfeiting principle diagram and the actual experimental device utilised for preparing flexible film items [104, 105].

These innovations collectively highlight the synergy between material design and dynamic optical control, paving the way for the development of next-generation adaptive devices for sensors, displays, and security technologies.

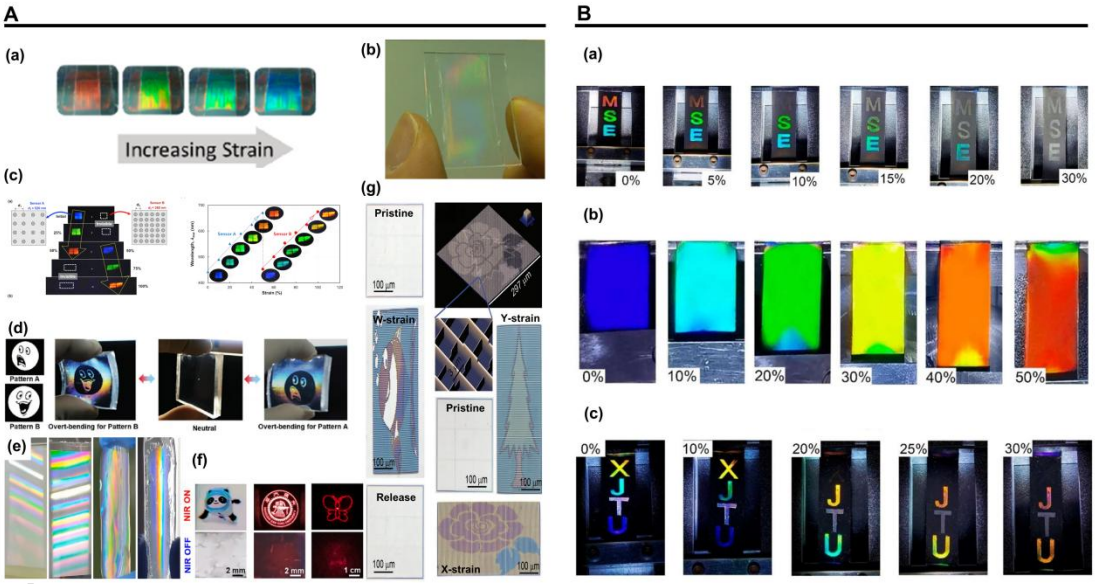

Fig. 11. Dynamic control technique of structural colour. (A) Dynamic control of structural colour patterns: (a) digital photos of 6-layer 1DPC showing colour shifts from red (0% strain) to blue (40% strain).[100] Reprinted from [100], Copyright (2015), with permission from American Chemical Society; (b) diffraction image of PMMA grating with 0.82 μm width.[106] Reprinted from [106], Copyright (2017), with permission from Elsevier. (c) Colour change of the strain sensor under tensile conditions.[103] Reprinted from [103], Copyright (2020), with permission from American Chemical Society; (d) device with

PDMS-encapsulated-SiO2-NP patterns displaying optical images under inward and outward bending.[101] John Wiley & Sons. © 2020 The Authors. Advanced Materials published by Wiley-VCH GmbH; (e) changes in photoresist, PDMS, and PUA grating templates after stretching and copying.[107] Reprinted from [107], Copyright (2021), with permission from Elsevier; (f) clear and fuzzy images dynamically obtained using the NIR on/off switch.[108] Reprinted from [108], Copyright (2022), with permission from Elsevier; (g) PDMS nano-grooves of varying depths achieve optical images. [64] **(B)** Reversible mechanical discoloration via surface fold manipulation.[109] Reprinted from [109] Copyright (2022), with permission from American Chemical Society. (a) Smart optical device by brightness mechanochromism (BM) strategy; letters "M", "S", and "E" disappear sequentially under stretching. (b) stretchable strain sensor (Hue Change Mechanochromism, HCM) attached to tensile specimen; colours shift from blue to red during tension; (c) anti-counterfeiting label stretched longitudinally; "X" and "T" fabricated by BM and viewable angle mechanochromism (VAM), "J" and "U" by HCM.

Nanoscale Imprinting and Lithography

Recent advancements in nanoscale imprinting and lithography have enabled the fabrication of dynamically tunable micro/nanostructures; however, challenges persist in terms of scalability, resolution, and adaptability.

As shown in **Fig. 12A(a)**, the translation stage serves as the core component of the experimental device for dynamic structural colour regulation. Based on this setup, a cost-effective PDMS-based nanograting technology can conveniently achieve dynamic control of the grating using elastic nanoforming techniques. The stimulus-response mechanism relies on the precise and reversible tuning of the grating period through uniaxial stretching of the PDMS substrate, governed by its controlled Poisson's ratio and elastic recovery. This method exhibits notable stability and repeatability across multiple stretching–replication cycles, maintaining structural fidelity and optical performance without significant degradation [106]. Although economically advantageous, its dependence on static moulds constrains its reconfigurability and geometric complexity.

To address these limitations, soft lithography techniques utilising PDMS moulds to

replicate biomimetic silicon nanocolumn arrays with programmable stiffness have been developed. This approach achieves stimulus-responsive geometric programming through controlled mechanical deformation of the elastic PDMS mould with intrinsic elasticity and precise parameter control, ensuring stable and repeatable performance across multiple cycles [110]. This approach successfully emulates natural functionalities, such as lotus-effect superhydrophobicity, but remains constrained by manual alignment requirements that impede manufacturing throughput.

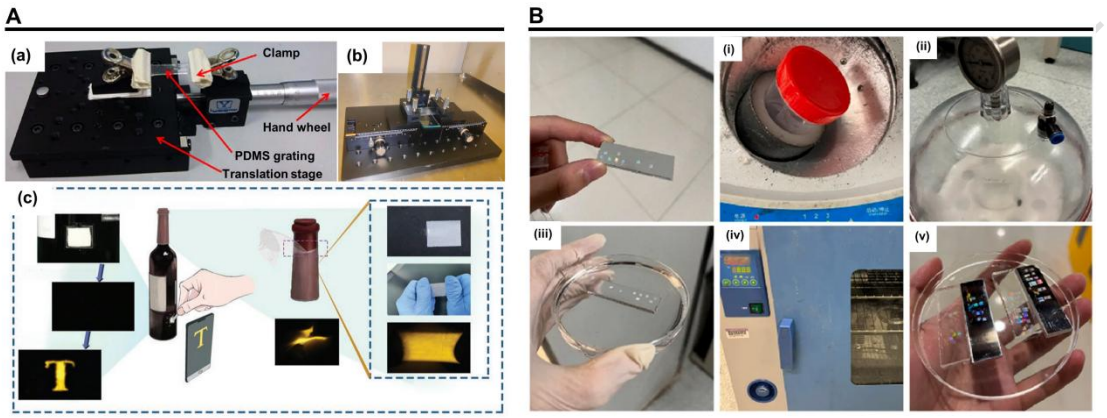

Fig. 12. Experimental device and process for dynamically regulating structural colour. **(A)** Experimental device for dynamically regulating structural colour: (a) translation stage;[106] (b) high-precision stretching-replication experiment platform;[107] (c) anti-counterfeiting principle diagram and actual experimental device for preparing flexible film items.[104, 105] John Wiley & Sons. © 2023 The Authors. Advanced Functional Materials, published by Wiley-VCH GmbH. **(B)** Process of transferring the metal 2D nanostructures template to the PDMS material.[111] Reprinted from [110], Copyright (2023), with permission from Elsevier. (i) Placing the prepared substrate and curing agent in a centrifuge for mixing; (ii) removing the bubbles by vacuum machine; (iii) blowing remaining bubbles away; (iv) drying the PDMS; (v) breaking the Petri dish and cutting the PDMS material.

To overcome throughput limitations, mechanical stretching-assisted nanoimprint lithography (NIL) enables dynamic grating period modulation, which demonstrates consistent stability and reproducibility under various environmental conditions owing to the elastic recovery and interfacial integrity of the hybrid mould. This approach circumvents the pattern-fidelity limitations of conventional lithography using

stretchable substrates, although material homogeneity requirements constrain multifunctional composite integration [112]. Expanding material versatility, flexible master mould nanoimprinting transfers grating architectures to PDMS films, achieving customised mid-infrared optical responses [113], with the stimulus–response behaviour of the grating-PDMS composite showing reliable performance under thermal and mechanical fluctuations. This is attributed to the robust adhesion and structural uniformity of the imprinted layers. However, this single-layer paradigm restricts multidimensional nanostructure fabrication. Both strategies represent trade-offs between scalability and functional complexity in dynamic nanostructuring.

Advancing beyond planar constraints, elliptical vibration nanoimprinting (EVN) enables rapid bidirectional nanostructuring on metallic surfaces, as shown in **Fig. 12B**. The strain-mediated reconstruction and photothermally driven mechanisms underpinning this technique demonstrate consistent stability under varying thermal and mechanical conditions, which is attributable to the controlled interfacial adhesion and precise trajectory control of the vibrating indenter. This technique facilitates anisotropic optical-response strain sensors, but faces interfacial adhesion challenges in metal-polymer transfers, compromising long-term stability [111].

Complementarily, mechanically stretched contact exposure and transfer printing optimise the PDMS grating templates, as shown in **Fig. 12A(b)**. The stimulus-response behaviour during stretching and replication exhibits reliable reproducibility across repeated cycles and environmental fluctuations owing to the viscoelastic recovery and structural fidelity of the PDMS-PUA composite system. While enhancing the linear grating density, this method exhibits inherent trade-offs: improved resolution comes at the expense of large-area uniformity owing to viscoelastic relaxation during processing [107].

These approaches collectively highlight the fundamental tension in dynamic nanostructuring: EVN achieves functional complexity but suffers from material limitations, whereas stretch-transfer methods prioritise resolution scalability at the cost of spatial consistency.

Ultimately, two-photon lithography (TPL) resolves the critical resolution-scalability trade-off through multiphoton polymerisation. The underlying strain-mediated grating reconstruction and photothermally driven nanocomposite mechanisms exhibit exceptional stability and reproducibility across numerous cycles, as demonstrated by highly reversible colour transitions maintained over 200 stretching/release operations. By fabricating precisely engineered cuboid grooves in PDMS, TPL enables reversible multistate colour switching with subdiffraction-limit precision. **Fig. 11A(g)** illustrates PDMS nanogrooves of varying depths that achieve tunable optical images. However, their dependence on ultrafast laser systems imposes significant fabrication costs [64]. This progression from nanoimprinting to TPL demonstrates a cumulative innovation pathway, in which each technology addresses the limitations of its predecessors in terms of scalability, material versatility, and dynamic control. Collectively, they establish adaptive nanomanufacturing platforms for next-generation optical encryption, high-sensitivity mechanosensors, and unforgeable security systems.

Photothermal and Mechanical Actuation

Hybrid photothermal-mechanical systems enable dynamic surface reconfiguration by converting optical energy into mechanical strain via photothermal effects; however, they face challenges in terms of scalability, spatial control, and long-term stability under multiphysics coupling. A representative photoresponsive wrinkling platform leverages carbon nanotube (CNT)-doped polydimethylsiloxane (PDMS) substrates to generate switchable metallic patterns upon near-infrared (NIR) light irradiation (**Fig. 11A(f)**) [108]. In this system, photothermal expansion induces compressive strains that dynamically modulate the wrinkle geometry. The quantitative relationship between incident light intensity (I), temperature rise (ΔT), induced thermal strain (ε_{th}), and consequent wrinkle amplitude (A) can be described as follows:

$$\varepsilon_{th} = \alpha \Delta T \approx \alpha \frac{\eta I A_{abs}}{h\kappa}$$

where α is the coefficient of thermal expansion (CTE) of the composite, η is the photothermal conversion efficiency of CNTs, A_{abs} is the absorbed light cross-section, h

is the film thickness, and κ is the thermal conductivity. Chen et al. demonstrated that under NIR irradiation (808 nm, 1.8 W/cm²), the temperature of a CNT-PDMS substrate rises rapidly above 100 °C, leading to wrinkle erasure within ~40 s. The recovery of wrinkles upon cooling follows a viscoelastic relaxation model, with the normalised amplitude (A/A_0) exhibiting repeatable decay and recovery over multiple NIR on/off cycles. This light–heat–strain–morphology coupling enables on-demand tunability; however, its stability and reproducibility under varying ambient conditions (e.g., humidity and baseline temperature) require further investigation. Moreover, localised heating constraints lead to non-uniform temperature fields, limiting the spatial uniformity and response kinetics in large-area implementations.

To overcome spatial resolution constraints, oxygen plasma-modified PDMS films, shown in **Fig. 11B**, enable three distinct mechanochromic responses through dynamic surface reconfiguration [109]. These films exhibit three distinct mechanochromic behaviours: stretch-induced hue shifts, angle-dependent iridescence, and pressure-responsive opacity changes.

The quantitative linkage between mechanical strain and optical response is rooted in the strain-dependent wrinkling dynamics. Wu et al. established that for brightness mechanochromism (BM), the wrinkle wavelength (d) remains nearly constant while the amplitude (A) decreases sharply with applied tensile strain (ε), following post-buckling mechanics. For hue-change mechanochromism (HCM), d increases significantly with ε, leading to a redshift in reflected wavelength ($\Delta\lambda$) according to Bragg's law. The gauge factor ($GF=\Delta\lambda/\lambda_0\varepsilon$) reaches ~1.0 over a 50% strain range, providing a quantitative metric for strain sensing.

However, plasma-induced surface embrittlement can lead to microcrack propagation under cyclic loading, degrading the mechanical durability and optical reversibility. The thermo-mechanical coupling in such systems—where variations in ambient temperature influence the Young's modulus of PDMS and, consequently, the strain–optical response—remains insufficiently explored and warrants systematic investigation under a range of environmental conditions.

Advancing toward localised control, microscale strain engineering has enabled pixel-level structural colour modulation through microlens array deformation. By precisely tuning the local lens widths via strain gradients, this method achieves pixel-level structural colour modulation for information encryption and wearable pressure mapping. While offering high spatial resolution, its scalability is hindered by the complexity of uniformly aligning microscale strain fields across large areas. Furthermore, the thermal expansion mismatch between different layers in such multimaterial systems can introduce unintended strain gradients under temperature fluctuations, affecting colour consistency and spatial fidelity.

Collectively, these innovations demonstrate cumulative breakthroughs in dynamic optical control, systematically overcoming historical constraints on spatial uniformity, cyclic durability, and fabrication scalability. Through strategic photothermal-mechanical synergy, this evolution has established new paradigms for sensing, security, and interactive interfaces. The integration of stimuli-responsive architectures with nanoscale precision enables the development of next-generation devices capable of real-time optical reconfiguration for critical applications. Future studies should focus on developing coupled photothermomechanical models that incorporate material nonlinearities, interfacial adhesion, and environmental factors to predict and enhance the operational stability of these dynamic systems under real-world multiphysics conditions.

Dynamic Regulation in Functional Devices

The integration of dynamically tunable optical architectures has expanded the capabilities of flexible electronics, although fundamental trade-offs persist between efficiency, scalability, and multifunctionality. Organic photovoltaics (OPVs) incorporating nanograting-patterned active layers demonstrate significantly enhanced power-conversion efficiency in ultraflexible configurations [114]. The stimulus-response dynamics of such static nanostructures under mechanical deformation and spectral shifts require a thorough examination to ensure their

stability and reproducible performance under real-world, variable conditions. Although transformative for energy harvesting, the static nature of these nanostructures fundamentally limits their real-time responsivity to mechanical deformation and spectral variation under changing environmental conditions.

To address these static limitations, stretchable wireless strain sensors employ conical plasmonic nanostructure arrays on elastomeric substrates, as shown in **Fig. 11A(d)**. Dynamic inter-nanostructure spacing modulation tunes localised surface plasmon resonances (LSPRs), generating colour-coded strain quantification. However, the nanofabrication complexity of high-density architectures substantially increases production costs and impedes scalable manufacturing.

To bridge this gap, soft-cast PDMS grating replication is a pragmatic alternative [101-103]. This method duplicates the commercial grating profiles for real-time force monitoring in flexible electronics and biomedical devices. While enabling accurate measurements at a minimal cost, its dependence on predefined patterns fundamentally restricts application-specific customisation, particularly for emerging spectral engineering requirements. Despite the demonstrated linear response under controlled conditions, the long-term stability and measurement reproducibility of these replicated gratings under varying environmental factors such as temperature, humidity, and mechanical fatigue remain unverified and warrant further systematic investigation. These contrasting approaches exemplify the core trade-off in dynamic sensing in that plasmonic systems offer nano-optical precision at scalability costs, whereas soft-replication prioritises accessibility over functional adaptability.

Collectively, this evolution demonstrates a strategic paradigm shift from static efficiency maximisation in OPVs to dynamic plasmonic strain responsiveness, culminating in cost-effective soft-replication solutions. Each breakthrough systematically addresses the core limitations of its predecessors, adaptability gaps, scalability barriers, and functional inflexibility through harmonised optomechanical engineering. By combining nanophotonic control with mechanical tunability, these technologies can fundamentally redefine the design principles of next-generation

adaptive devices.

Structural Colour-RIS Integration Study

The advancement of PDMS-based dynamic regulation technologies depends on rigorous material property quantification and predictive modelling. Plane stamping indentation experiments combined with multiphysics finite element simulations were employed to systematically investigate the mechanical and optical responses of thin PDMS films under controlled stress states. These investigations quantified critical parameters, including the elastic modulus, strain-dependent light transmission, and stress-strain hysteresis, providing essential data for predicting and optimising PDMS behaviour in dynamic environments. For instance, simulations revealed the correlation between compressive strain gradients and optical birefringence in PDMS, enabling precise predesign of structural colour shifts under mechanical loading.

Complementary progress in auxiliary functional materials has further expanded the tunability of dynamic optical systems. Liquid crystal composites integrated with PDMS have demonstrated enhanced response kinetics via orientation-dependent refractive index modulation, while nanoparticle doping has been shown to tailor the mechanical stiffness and resonance design resonance of PDMS, thereby augmenting spectral adjustability and sensing sensitivity.

However, while these controlled studies have established fundamental correlations, the long-term stability and reproducible stimulus-response behaviour of such strain-modulated optical properties under varying environmental conditions require further systematic investigation. Such insights are pivotal for designing adaptive devices, such as stretchable optical sensors or mechanically reconfigurable displays, where real-time modulation relies on predictable material performance [115].

Recent advancements in reconfigurable intelligent surfaces (RIS) are transcending this traditional trade-off by integrating dynamically tunable structural colours with secure wireless communication protocols. This convergence enables functional devices that are not only responsive, but also capable of actively encoding and transmitting information. For instance, RIS-empowered noncoherent chaotic

communication systems leverage the real-time phase-modulation capabilities of RIS to manipulate structural colour-based signals. One approach utilises two-level nested index modulation (TLNIM) with differential chaos-shift keying (DCSK), doubling spectral efficiency and improving bit-error-rate performance by over 6 dB without requiring channel state information. [116] Another approach employs RIS-enabled M-ary DCSK with block interleaving (BI), which utilises chaotic merging and sorting algorithms to generate encryption patterns. This method ensures high security, with eavesdropped information leakage below 0.1 bit and an error rate approaching 0.5 for unauthorized receivers, while achieving a gain exceeding 2 dB in bit-error-rate performance over benchmark systems. [117] These RIS-driven platforms address the functional limitations of existing dynamic colour devices by transforming them into secure and adaptive interfaces for information transmission, thereby opening new avenues for high-security anti-counterfeiting, optical encryption, and covert communication.

By bridging experimental validation with computational modelling, this study established a robust framework for tailoring PDMS properties to meet the demands of next-generation dynamic optical systems. **Table 4** presents a comparison of the processing methods for dynamic optical systems, summarising key performance metrics of each technical route to provide an intuitive reference for practical application selection.

Table 4 Quantitative comparison of processing methods for dynamic optical systems

Processing Method	**Relative Response Time**	**Cyclic Durability**	**Energy Efficiency**
PDMS Grating Soft Casting	Millisecond-level	Stable for >1000 cyclic bends; elastic modulus retention >90% after cyclic loading	Passive (no external energy required); low energy consumption (only mechanical work for strain)
PDMS Thin Film	Millisecond to second-level	Stable for >1000 cycles (strain <50%); no significant structural damage	Passive (mechanical stress-driven); no extra energy input

PDMS-Liquid Crystal Composite	Millisecond-level	500-1000 stable cycles; minor liquid crystal orientation degradation over time	Passive (orientation-dependent refractive index modulation); low energy consumption
Nanoparticle-doped PDMS (SiO_2/Metal NPs)	Millisecond-level	>1000 stable cycles; no particle detachment or structural cracking	Passive (plasmonic resonance/mechanical tuning); no external energy needed
Nanograting-patterned OPV	Millisecond to second-level	900 compression cycles (33% strain); PCE retention ~74.6% (from 9.82% to 7.33%)	Active (self-powered); PCE up to 10.5%, power-per-weight 11.46 W/g
Conical Plasmonic Nanostructure Array	Millisecond-level	>1000 cycles; Peak wavelength SD: 3.35 nm (relaxed) / 0.68 nm (50% strain)	Passive (mechanical strain-driven); no external energy
RIS-Integrated Structural Colour (TLNIM-DCSK)	Microsecond to millisecond-level	>1000 modulation cycles; BER performance stable	Active (low energy for phase modulation); spectral efficiency doubled
RIS-Integrated Structural Colour (M-ary DCSK-BI)	Microsecond to millisecond-level	>1000 encoding cycles; information leakage <0.1 bit	Active (low energy for chaos coding); BER gain >2 dB over benchmarks

Conclusion and future perspectives

This review comprehensively surveys the burgeoning research landscape of structural colours within materials science, with a dedicated focus on pivotal fabrication techniques for nanostructures and their transformative application in dynamic colour control. Distinguished from conventional pigments owing to their superior colour persistence, environmental benignity, and remarkable tunability, structural colours represent a paradigm shift toward advanced material design and functionality.

Commencing with the fundamental principles underpinning structural colours, we underscore their compelling advantages, particularly in terms of longevity, eco-friendliness, and dynamic modulation capabilities, separating them from traditional colouring agents.

Subsequently, a detailed examination of diverse fabrication methodologies is presented. Advanced micro/nano-machining techniques enable precise sculpting of material surfaces at the nanoscale, yielding tailored structural features responsible for specific and vibrant colour generation. Complementing these, nonmechanical fabrication approaches, including laser processing and lithography, have emerged as powerful tools to open new frontiers, particularly for achieving large-area, scalable, and potentially low-cost production of structurally coloured surfaces.

Critically, the integration of these sophisticated nanostructures with stimuli-responsive materials not only advances dynamic colour-tuning technologies, but also forges a tight link with smart surface applications. This integration enables smart surfaces with adaptive optical functionalities. For instance, self-regulating displays that adjust to ambient light or anticounterfeiting surfaces with reversible colour shifts address the underdeveloped connection between structural colour engineering and smart surface utility.

The evolution of structural colour research hinges on several key trajectories, each directly tied to the critical gaps identified in this review.

First, the pursuit of novel, cost-effective, and environmentally sustainable fabrication strategies must target the throughput limitations of current mechanical and nonmechanical methods. As highlighted in the fabrication section, future work should develop AI-driven toolpath algorithms for mechanical processing (e.g., single-point diamond turning) and high-efficiency laser ablation protocols for nonmechanical techniques to overcome scalability bottlenecks while maintaining structural precision.

Second, deepening the fundamental understanding of light-matter interactions within complex, multiscale, and responsive nanostructures is crucial, especially to address the gap in multiscale structural co-design identified earlier. This requires advanced simulation tools that couple micro-scale structural geometry with nanoscale light modulation effects, enabling precise prediction and design of novel optical properties tailored to specific applications.

Third, exploring innovative mechanisms and materials for achieving ultrafast,

wide-gamut, and reversible dynamic colour modulation must build on the limitations of existing dynamic regulation systems. The dynamic modulation section reveals the critical need for new composite materials that combine the speed of photothermal actuation with the durability of mechanical systems (e.g., strain-induced lattice adjustments), enabling reliable performance under diverse stimuli (electrical, optical, thermal, and chemical) for real-world deployment.

Finally, bridging the gap between laboratory-scale achievements and real-world applications necessitates focused efforts to enhance the mechanical robustness and long-term environmental stability, two underdeveloped aspects highlighted earlier. This includes developing protective coatings for nanostructures to resist wear and environmental erosion as well as seamless integration strategies that adapt structural colour modules to existing smart device architectures (e.g., wearable electronics and adaptive displays).

Addressing these challenges will undoubtedly unlock the full potential of structural colours, paving the way for revolutionary applications in photonics, sensing, anti-counterfeiting, and adaptive camouflage.

CRediT authorship contribution statement

Lin Zhang: Funding acquisition, Writing - review & editing. **Caixia Zhang**: Writing - original draft, Visualization, Software, Validation, Investigation. **Yang Yang**: Methodology, Formal analysis, Reviewer response, Writing – revision. **Jieqiong Lin**: Resources, Project administration. **Jiwang Yan**: Conceptualization, Supervision.

Declaration of Competing Interest

The authors declare that they have no known competing financial interests or personal relationships that may have influenced the work reported in this paper.

Data availability

Data will be made available on request.

Acknowledgement

This research was funded by the National Natural Science Foundation of China (Grant Nos. 52305445 and 22FAA01871) and Science and Technology Development Plan Project of Jilin Province (Grant No. YDZJ202401338ZYTS), Research Project of State Key Laboratory of Mechanical Systems and Vibration (Grant No. MSV202412).

References

1. Xuan, Z. Y. et al. Artificial structural colors and applications. *The Innovation* **2**, 100081 (2021) doi: 10.1016/j.xinn.2021.100081.

2. Born, M., Wolf, E. & Hecht, E. Principles of optics: electromagnetic theory of propagation, interference and diffraction of light. *Physics Today* **53**, 77-78 (2000) doi: 10.1063/1.1325200.

3. Finet, C. Light as matter: natural structural colour in art. *Humanities and Social Sciences Communications* **10**, 348 (2023) doi: 10.1057/s41599-023-01854-0.

4. Fu, Y. L. et al. Structural colors: from natural to artificial systems. *WIREs Nanomedicine and Nanobiotechnology* **8**, 758-775 (2016) doi: 10.1002/wnan.1396.

5. Goodling, A. E. et al. Colouration by total internal reflection and interference at microscale concave interfaces. *Nature* **566**, 523-527 (2019) doi: 10.1038/s41586-019-0946-4.

6. Ito, M. M. et al. Structural colour using organized microfibrillation in glassy polymer films. *Nature* **570**, 363-367 (2019) doi: 10.1038/s41586-019-1299-8.

7. Shang, L. R. et al. Bio-inspired intelligent structural color materials. *Materials Horizons* **6**, 945-958 (2019) doi: 10.1039/C9MH00101H.

8. Yuan, L. et al. Synthesis and characterization of environmentally benign inorganic pigments with high NIR reflectance: lanthanum-doped $BiFeO_3$. *Dyes and Pigments* **148**, 137-146 (2018) doi: 10.1016/j.dyepig.2017.09.008.

9. Wang, Z. Y. et al. Mass fabrication of hierarchical nanostructures based on plasmonic nanochemistry for ultra-sensitive optical sensing. *Sensors and Actuators B*: *Chemical* **329**, 129220 (2021) doi: 10.1016/j.snb.2020.129220.

10. Cuthill, I. C. et al. The biology of color. *Science* **357**, eaan0221 (2017) doi: 10.1126/science.aan0221.

11. Ghiradella, H. Light and color on the wing: structural colors in butterflies and moths. *Applied Optics* **30**, 3492-3500 (1991) doi:

10.1364/AO.30.003492.

12. Wu, P. P., Wang, J. X. & Jiang, L. Bio-inspired photonic crystal patterns. *Materials Horizons* **7**, 338-365 (2020) doi: 10.1039/C9MH01389J.

13. Chen, K. et al. Bioinspired dynamic camouflage from colloidal nanocrystals embedded electrochromics. *Nano Letters* **21**, 4500-4507 (2021) doi: 10.1021/acs.nanolett.1c01419.

14. Yang, B. et al. Ultrahighly saturated structural colors enhanced by multipolar-modulated metasurfaces. *Nano Letters* **19**, 4221-4228 (2019) doi: 10.1021/acs.nanolett.8b04923.

15. Vukusic, P. & Sambles J. R. Photonic structures in biology. *Nature* **424**, 6950 (2003) doi: 10.1038/nature01941.

16. Teyssier, J. et al. Photonic crystals cause active colour change in chameleons. *Nature Communications* **6**, 6368 (2015) doi: 10.1038/ncomms7368.

17. Fu, F. F. et al. Bioinspired living structural color hydrogels. *Science Robotics* **3**, eaar8580 (2018) doi: 10.1126/scirobotics.aar8580.

18. Feng, L. et al. Review of recent advancements in the biomimicry of structural colors. *Dyes and Pigments* **210**, 111019 (2023) doi: 10.1016/j.dyepig.2022.111019.

19. Li, Y. J. et al. Recent progress on structural coloration. *Photonics Insights* **3**, R03 (2024) doi: 10.3788/PI.2024.R03.

20. Schift, H. Nanoimprint lithography: an old story in modern times? A review. *Journal of Vacuum Science & Technology B*: *Microelectronics and Nanometer Structures Processing*, *Measurement*, *and Phenomena* **26**, 458-480 (2008) doi: 10.1116/1.2890972.

21. Xiong, K. L. et al. Active control of plasmonic colors: emerging display technologies. *Reports on Progress in Physics* **82**, 024501 (2019) doi: 10.1088/1361-6633/aaf844.

22. Qi, Y., Zhang, S. F. & Lu, A. H. Responsive structural colors derived from geometrical deformation of synthetic nanomaterials. *Small Structures* **3**,

2200101 (2022) doi: 10.1002/sstr.202200101.

23. Chen, F. X. et al. Bio-inspired structural colors and their applications. *Chemical Communications* **57**, 13448-13464 (2021) doi: 10.1039/D1CC04386B.

24. Yang, W. H. et al. All-dielectric metasurface for high-performance structural color. *Nature Communications* **11**, 1864 (2020) doi: 10.1038/s41467-020-15773-0.

25. Lin, X. F. et al. Structural color‐based physical unclonable function. *Responsive Materials* **2**, e20230031 (2024) doi: 10.1002/rpm.20230031.

26. Zhang, W. H. et al. Structural color colloidal photonic crystals for biomedical applications. *Advanced Science* **11**, 2403173 (2024) doi: 10.1002/advs.202403173.

27. Zhang, S. J. et al. Advances in ultra-precision machining of micro-structured functional surfaces and their typical applications. *International Journal of Machine Tools and Manufacture* **142**, 16-41 (2019) doi: 10.1016/j.ijmachtools.2019.04.009.

28. Duan, H. G. et al. Direct and reliable patterning of plasmonic nanostructures with sub-10-nm gaps. *ACS Nano* **5**, 7593-7600 (2011) doi: 10.1021/nn2025868.

29. Kaplan, A. F., Xu, T. & Guo, L. J. High efficiency resonance-based spectrum filters with tunable transmission bandwidth fabricated using nanoimprint lithography. *Applied Physics Letters* **99**, 143111 (2011) doi: 10.1063/1.3647633.

30. Lee, Y. C. et al. Enhanced light trapping based on guided mode resonance effect for thin-film silicon solar cells with two filling-factor gratings. *Optics Express* **16**, 7969-7975 (2008) doi: 10.1364/OE.16.007969.

31. Ding, X. & Rahman, M. A study of the performance of cutting polycrystalline Al 6061 T6 with single crystalline diamond micro-tools. *Precision Engineering* **36**, 593-603 (2012) doi: 10.1016/j.precisioneng.2012.04.009.

32. Ding, X. et al. A study of the cutting performance of poly-crystalline oxygen free copper with single crystalline diamond micro-tools. *Precision Engineering* **36**, 141-152 (2012) doi: 10.1016/j.precisioneng.2011.09.001.

33. Tang, L. L. et al. Research on single point diamond turning of chalcogenide glass aspheric lens. *Procedia CIRP* **71**, 293-298 (2018) doi: 10.1016/j.procir.2018.05.023.

34. Cao, J. G. et al. Material removal behavior in ultrasonic-assisted scratching of SiC ceramics with a single diamond tool. *International Journal of Machine Tools and Manufacture* **79**, 49-61 (2014) doi: 10.1016/j.ijmachtools.2014.02.002.

35. To, S., Lee, W. B. & Chan, C. Y. Ultraprecision diamond turning of aluminium single crystals. *Journal of Materials Processing Technology* **63**, 157-162 (1997) doi: 10.1016/S0924-0136(96)02617-9.

36. Zhang, G. Q., Dai, Y. Q. & Lai, Z. H. A novel force-based two-dimensional tool centre error identification method in single-point diamond turning. *Precision Engineering* **70**, 92-109 (2021) doi: 10.1016/j.precisioneng.2021.01.019.

37. Huang, R. et al. Ultra-precision machining of grayscale pixelated micro images on metal surface. *Precision Engineering* **52**, 211-220 (2018) doi: 10.1016/j.precisioneng.2017.12.009.

38. Huang, R. et al. An innovative method of machining freeform feature based on digital image by fast tool servo diamond turning. Proceedings of the 4th International & 25th All India Manufacturing Technology, Design and Research Conference (AIMTDR 2012). Kolkata, West Bengal, India: AIMTDR, 2012.

39. Li, D. Y. et al. Diamond machining of optical functional surface. Proceedings of the 20th International Conference of the European Society for Precision Engineering and Nanotechnology. Geneva, Switzerland: EUSPEN 2020, 2020, 2 p.

40. Wang, J. J. et al. Structural coloration of non-metallic surfaces using

ductile-regime vibration-assisted ultraprecision texturing. *Light*: *Advanced Manufacturing* **2**, 434-445 (2021) doi: 10.37188/lam.2021.033.

41. Wang, J. J. et al. Blazed grating enables highly decoupled optically variable devices fabricated by vibration-assisted diamond texturing. *Optics Express* **30**, 8829-8846 (2022) doi: 10.1364/OE.450628.

42. Du, H. H. et al. Development and assessment of a novel two-degree-of-freedom vibration generator for generating and hiding optical information. *Mechanical Systems and Signal Processing* **181**, 109470 (2022) doi: 10.1016/j.ymssp.2022.109470.

43. Wang, Y. K., Landis, M. & Guo, P. Nanometric surficial reflectors: achieving high‐performance and high‐throughput structural coloration through modulation‐assisted machining. *Advanced Science* **13**, e06162 (2026) doi: 10.1002/advs.202506162.

44. Ding, P. Y. et al. Fabrication of optical Fourier surface by multiple‐frequency vibration cutting for structural true coloration. *Small* **19**, 2303500 (2023) doi: 10.1002/smll.202303500.

45. Chen, Z. M. et al. Shaped vibration cutting: a novel fabrication method for mid-infrared relief gratings with controllable profiles. *Journal of Materials Processing Technology* **317**, 118007 (2023) doi: 10.1016/j.jmatprotec.2023.118007.

46. Lin, C. C. & Yang, Y. Effect of tool vibration trajectory on vibration-assisted diamond-cutting structural color. *International Journal of Mechanical Sciences* **280**, 109632 (2024) doi: 10.1016/j.ijmecsci.2024.109632.

47. Suzuki, N., Yokoi, H. & Shamoto, E. Micro/Nano sculpturing of hardened steel by controlling vibration amplitude in elliptical vibration cutting. *Precision Engineering* **35**, 44-50 (2011) doi: 10.1016/j.precisioneng.2010.09.006.

48. Yang, Y., Lin, R. X. & Zhao, Z. J. Deterministic rendering of structural color induced by atypical nano-gratings in ultra-precision diamond cutting.

Applied Surface Science **638**, 158065 (2023) doi: 10.1016/j.apsusc.2023.158065.

49. Yang, Y., Pan, Y. Y. & Guo, P. Structural coloration of metallic surfaces with micro/nano-structures induced by elliptical vibration texturing. *Applied Surface Science* **402**, 400-409 (2017) doi: 10.1016/j.apsusc.2017.01.026.

50. Wang, J. J. et al. Fabrication of structurally colored basso-relievo with modulated elliptical vibration texturing. *Precision Engineering* **64**, 113-121 (2020) doi: 10.1016/j.precisioneng.2020.03.021.

51. Wang, J. J. et al. Modulated vibration texturing of hierarchical microchannels with controllable profiles and orientations. *CIRP Journal of Manufacturing Science and Technology* **30**, 58-67 (2020) doi: 10.1016/j.cirpj.2020.04.002.

52. Ding, P. Y. et al. Portable machine tools by small piezoelectric robots for scalable and waviness‐adaptive fabrication of surface microstructures. *Advanced Intelligent Systems* **7**, 2400322 (2025) doi: 10.1002/aisy.202400322.

53. Yang, Y. & Guo, P. Fast generation of planar microstructured surfaces by elliptical vibration texturing. *Journal of Micro and Nano-Manufacturing* **5**, 011004 (2017) doi: 10.1115/1.4035390.

54. Li, Z. W. et al. Elliptical vibration chiseling: a novel process for texturing ultra-high-aspect-ratio microstructures on the metallic surface. *International Journal of Extreme Manufacturing* **6**, 025102 (2024) doi: 10.1088/2631-7990/ad1bbb.

55. He, Y. P. et al. Generation of high-saturation two-level iridescent structures by vibration-assisted fly cutting. *Materials & Design* **193**, 108839 (2020) doi: 10.1016/j.matdes.2020.108839.

56. He, Y. P. et al. Diffraction manipulation of visible light with submicron structures for structural coloration fabrication. *Optics Express* **29**, 9294-9311 (2021) doi: 10.1364/OE.419291.

57. He, Y. P. et al. Theoretical and experimental investigation on the

radial-fly-cutting process for micro-structured surface fabrication. *Journal of Materials Processing Technology* **310**, 117785 (2022) doi: 10.1016/j.jmatprotec.2022.117785.

58. Chen, Z. Q. et al. High-precision and high-efficiency fabrication of blazed grating by ultrasonic-assisted ultraprecision planing. *Journal of Materials Processing Technology* **311**, 117802 (2023) doi: 10.1016/j.jmatprotec.2022.117802.

59. Zheng, Z. P. et al. Controllable fabrication of microstructures on the metallic surface using oblique rotary ultrasonic milling. *International Journal of Mechanical Sciences* **237**, 107805 (2023) doi: 10.1016/j.ijmecsci.2022.107805.

60. Zhou, T. F. et al. Algorithm of micro-grooving and imaging processing for the generation of high-resolution structural color images. *Nanomanufacturing and Metrology* **3**, 187-198 (2020) doi: 10.1007/s41871-020-00068-1.

61. He, Y. P. et al. Three-level nanogrooves by vibration-assisted fly-cutting for diffraction regulation and array output. *Optics Letters* **47**, 2730-2733 (2022) doi: 10.1364/OL.459748.

62. Han, S. et al. Lithographically encoded polymer microtaggant using high‐capacity and error‐correctable QR code for anti‐counterfeiting of drugs. *Advanced Materials* **24**, 5924-5929 (2012) doi: 10.1002/adma.201201486.

63. Chen, L. N. et al. Large‐area patterning of metal nanostructures by dip‐pen nanodisplacement lithography for optical applications. *Small* **13**, 1702003 (2017) doi: 10.1002/smll.201702003.

64. Ruan, Q. F. et al. Reconfiguring colors of single relief structures by directional stretching. *Advanced Materials* **34**, 2108128 (2022) doi: 10.1002/adma.202108128.

65. Zhang, W. et al. Structural multi-colour invisible inks with submicron 4D printing of shape memory polymers. *Nature Communications* **12**, 112 (2021)

doi: 10.1038/s41467-020-20300-2.

66. Zhang, W. et al. Stiff shape memory polymers for high-resolution reconfigurable nanophotonics. *Nano Letters* **22**, 8917-8924 (2022) doi: 10.1021/acs.nanolett.2c03007.

67. Huang, L. Y. et al. Sub-wavelength patterned pulse laser lithography for efficient fabrication of large-area metasurfaces. *Nature Communications* **13**, 5823 (2022) doi: 10.1038/s41467-022-33644-8.

68. Chan, J. Y. E. et al. Full geometric control of hidden color information in diffraction gratings under angled white light illumination. *Nano Letters* **22**, 8189-8195 (2022) doi: 10.1021/acs.nanolett.2c02741.

69. Rubahn, K. et al. UV laser-induced grating formation in PDMS thin films. *Applied Physics A* **79**, 1715-1719 (2004) doi: 10.1007/s00339-004-2888-3.

70. Liu, H. G., Lin, W. X. & Hong, M. H. Surface coloring by laser irradiation of solid substrates. *APL Photonics* **4**, 051101 (2019) doi: 10.1063/1.5089778.

71. Vorobyev, A. Y. & Guo, C. L. Colorizing metals with femtosecond laser pulses. *Applied Physics Letters* **92**, 041914 (2008) doi: 10.1063/1.2834902.

72. Geng, J. et al. High-speed laser writing of structural colors for full-color inkless printing. *Nature Communications* **14**, 565 (2023) doi: 10.1038/s41467-023-36275-9.

73. Ou, Z. G., Huang, M. & Zhao, F. L. Colorizing pure copper surface by ultrafast laser-induced near-subwavelength ripples. *Optics Express* **22**, 17254-17265 (2014) doi: 10.1364/OE.22.017254.

74. Nauval, F. et al. Diffraction and interference pattern by 4f imaging system to determine the thin film magnetic properties. *Journal of Physics*: *Conference Series* **1317**, 012054 (2019) doi: 10.1088/1742-6596/1317/1/012054.

75. Fantova, J. et al. Single-step fabrication of highly tunable blazed gratings using triangular-shaped femtosecond laser pulses. *Micromachines* **15**,

711 (2024) doi: 10.3390/mi15060711.

76. Mu, M. et al. In situ growth of laser-induced graphene on flexible substrates for wearable sensors. *ACS Applied Nano Materials* **7**, 3279-3288 (2024) doi: 10.1021/acsanm.3c05669.

77. Li, X. R. et al. Laser-based bionic manufacturing. *International Journal of Extreme Manufacturing* **6**, 042003 (2024) doi: 10.1088/2631-7990/ad3f59.

78. Chowdhury, D., Paul, A. & Chattopadhyay, A. Patterning design in color at the submicron scale. *Nano Letters* **1**, 409-412 (2001) doi: 10.1021/nl0155678.

79. Zhang, X. et al. Magnetron sputtering deposition of Ag/Ag_2O bilayer films for highly efficient color generation on fabrics. *Ceramics International* **46**, 13342-13349 (2020) doi: 10.1016/j.ceramint.2020.02.113.

80. You En Chan, J., Ruan, Q. F. & Yang, J. K. W. Structural color prints combined with microlens arrays for sustainable autostereoscopic displays. *Materials Today*: *Proceedings* **70**, 283-288 (2022) doi: 10.1016/j.matpr.2022.09.239.

81. Zhao, C. F. et al. Research progress on the design of structural color materials based on 3D printing. *Advanced Materials Technologies* **8**, 2200257 (2023) doi: 10.1002/admt.202200257.

82. Heydari, E. et al. Plasmonic color filters as dual‐state nanopixels for high‐density microimage encoding. *Advanced Functional Materials* **27**, 1701866 (2017) doi: 10.1002/adfm.201701866.

83. Knop, K. Rigorous diffraction theory for transmission phase gratings with deep rectangular grooves. *Journal of the Optical Society of America* **68**, 1206-1210 (1978) doi: 10.1364/JOSA.68.001206.

84. Schueller, O. J. A. et al. Reconfigurable diffraction gratings based on elastomeric microfluidic devices. *Sensors and Actuators A*: *Physical* **78**, 149-159 (1999) doi: 10.1016/S0924-4247(98)00242-8.

85. Görrn, P. & Wagner, S. Topographies of plasma-hardened surfaces of poly(dimethylsiloxane). *Journal of Applied Physics* **108**, 093522 (2010) doi:

10.1063/1.3482020.

86. Wu, K. et al. Two-stage wrinkling of Al films deposited on polymer substrates. *Scripta Materialia* **162**, 456-459 (2019) doi: 10.1016/j.scriptamat.2018.12.016.

87. Kumar, K. et al. Printing colour at the optical diffraction limit. *Nature Nanotechnology* **7**, 557-561 (2012) doi: 10.1038/nnano.2012.128.

88. Zhu, X. L. et al. Plasmonic colour laser printing. *Nature Nanotechnology* **11**, 325-329 (2016) doi: 10.1038/nnano.2015.285.

89. Yue, W. J. et al. Subtractive color filters based on a silicon-aluminum hybrid-nanodisk metasurface enabling enhanced color purity. *Scientific Reports* **6**, 29756 (2016) doi: 10.1038/srep29756.

90. James, T. D., Mulvaney, P. & Roberts, A. The plasmonic pixel: large area, wide gamut color reproduction using aluminum nanostructures. *Nano Letters* **16**, 3817-3823 (2016) doi: 10.1021/acs.nanolett.6b01250.

91. Højlund-Nielsen, E. et al. Plasmonic colors: toward mass production of metasurfaces. *Advanced Materials Technologies* **1**, 1600054 (2016) doi: 10.1002/admt.201600054.

92. Franklin, D. et al. Polarization-independent actively tunable colour generation on imprinted plasmonic surfaces. *Nature Communications* **6**, 7337 (2015) doi: 10.1038/ncomms8337.

93. Wang, G. P. et al. Mechanical chameleon through dynamic real-time plasmonic tuning. *ACS Nano* **10**, 1788-1794 (2016) doi: 10.1021/acsnano.5b07472.

94. Tseng, M. L. et al. Two-dimensional active tuning of an aluminum plasmonic array for full-spectrum response. *Nano Letters* **17**, 6034-6039 (2017) doi: 10.1021/acs.nanolett.7b02350.

95. Kumagai, H. et al. Stretchable and high‐adhesive plasmonic metasheet using al subwavelength grating embedded in an elastomer nanosheet. *Advanced Optical Materials* **8**, 1902074 (2020) doi: 10.1002/adom.201902074.

96. Huang, C. et al. Controllable structural colored screen for real-time display via near-infrared light. *ACS Applied Materials & Interfaces* **12**, 20867-20873 (2020) doi: 10.1021/acsami.0c03213.

97. Hosokawa, K., Hanada, K. & Maeda, R. A polydimethylsiloxane (PDMS) deformable diffraction grating for monitoring of local pressure in microfluidic devices. *Journal of Micromechanics and Microengineering* **12**, 1-6 (2002) doi: 10.1088/0960-1317/12/1/301.

98. Hosokawa, K. & Maeda, R. In-line pressure monitoring for microfluidic devices using a deformable diffraction grating. Proceedings of the Technical Digest. MEMS 2001. 14th IEEE International Conference on Micro Electro Mechanical Systems (Cat. No.01CH37090). Interlaken, Switzerland: IEEE, 2001, 174-177.

99. Hong, S. et al. Highly stretchable and transparent metal nanowire heater for wearable electronics applications. *Advanced Materials* **27**, 4744-4751 (2015) doi: 10.1002/adma.201500917.

100. Howell, I. R. et al. Strain-tunable one dimensional photonic crystals based on zirconium dioxide/slide-ring elastomer nanocomposites for mechanochromic sensing. *ACS Applied Materials & Interfaces* **7**, 3641-3646 (2015) doi: 10.1021/am5079946.

101. Zhou, Q. T. et al. Multimodal and covert–overt convertible structural coloration transformed by mechanical stress. *Advanced Materials* **32**, 2001467 (2020) doi: 10.1002/adma.202001467.

102. Jin, C. Y. et al. A force measurement method based on flexible PDMS grating. *Applied Sciences* **10**, 2296 (2020) doi: 10.3390/app10072296.

103. Quan, Y. J. et al. Stretchable biaxial and shear strain sensors using diffractive structural colors. *ACS Nano* **14**, 5392-5399 (2020) doi: 10.1021/acsnano.9b08953.

104. Li, L. P. et al. Stress‐triggered mechanoluminescence in ZnO‐based heterojunction for flexible and stretchable mechano‐optics. *Advanced Functional Materials* **33**, 2301372 (2023) doi: 10.1002/adfm.202301372.

105. Ke, Y. J. et al. Engineering dynamic structural color pixels at microscales by inhomogeneous strain-induced localized topographic change. *Nano Letters* **23**, 5520-5527 (2023) doi: 10.1021/acs.nanolett.3c00808.

106. Zhang, B. Z. et al. A new fabrication method for nano-gratings based on the high flexibility of PDMS. *Optics & Laser Technology* **92**, 206-210 (2017) doi: 10.1016/j.optlastec.2016.12.030.

107. Jin, J. et al. A method to increase line-density of grating based on PDMS stretching and PUA replication process. *Microelectronic Engineering* **247**, 111586 (2021) doi: 10.1016/j.mee.2021.111586.

108. Chen, S. et al. Dynamic metal patterns of wrinkles based on photosensitive layers. *Science Bulletin* **67**, 2186-2195 (2022) doi: 10.1016/j.scib.2022.10.016.

109. Wu, K. et al. Reversible mechanochromisms via manipulating surface wrinkling. *Nano Letters* **22**, 2261-2269 (2022) doi: 10.1021/acs.nanolett.1c04494.

110. Pokroy, B. et al. Fabrication of bioinspired actuated nanostructures with arbitrary geometry and stiffness. *Advanced Materials* **21**, 463-469 (2009) doi: 10.1002/adma.200801432.

111. Zhang, H. W. et al. Structural coloration with two-dimensional nanostructures fabricated by elliptical vibration nanoindentation. *Precision Engineering* **82**, 219-232 (2023) doi: 10.1016/j.precisioneng.2023.03.018.

112. Qian, M. C. et al. Tuning the period of nanogratings using mechanical stretching and nanoimprint lithography. *Applied Physics A* **122**, 577 (2016) doi: 10.1007/s00339-016-0106-8.

113. Song, J. et al. Ultrahigh emissivity of grating-patterned PDMS film from 8 to 13 *μ*m wavelength regime. *Applied Physics Letters* **117**, 094101 (2020) doi: 10.1063/5.0017838.

114. Park, S. et al. Self-powered ultra-flexible electronics via nano-grating-patterned organic photovoltaics. *Nature* **561**, 516-521 (2018) doi: 10.1038/s41586-018-0536-x.

115. Park, J. S. et al. Investigating the mechanical and optical properties of thin PDMS film by flat-punched indentation. *Optical Materials* **85**, 153-161 (2018) doi: 10.1016/j.optmat.2018.08.051.

116. Cai, X. M. et al. Design of non-coherent RIS-empowered DCSK with two-level nested index modulation. *IEEE Transactions on Wireless Communications* **24**, 3044-3058 (2025) doi: 10.1109/TWC.2025.3527499.

117. Cai, X. M. et al. Toward chaotic secure communications: an RIS enabled *M*-ary differential chaos shift keying system with block interleaving. *IEEE Transactions on Communications* **71**, 3541-3558 (2023) doi: 10.1109/TCOMM.2023.3262834.